Project: RFP # FAAA 2016000120 (FRAPPÉ and DISCOVER-AQ Data Analysis)

Final Report, July 2017

Process-Based and Regional Source Impact Analysis for FRAPPÉ and DISCOVER-AQ 2014

Principal Investigators: Gabriele Pfister, Frank Flocke
Co-Investigators: Rebecca Hornbrook, John Orlando
Post-Doc: Sojin Lee
With contributions by Jason Schroeder, NASA Langley Research Center

National Center for Atmospheric Research (NCAR)
Atmospheric Chemistry Observations and Modeling Laboratory (ACOM)
3450 Mitchell Lane, Boulder CO 80301

Date: 31 July 2017

Overview

Two major field campaigns – the National Science Foundation (NSF)/National Center for Atmospheric Research (NCAR) and State of Colorado Front Range Air Pollution and Photochemistry Éxperiment (FRAPPÉ) and the 4th deployment of the National Aeronautics and Space Administration (NASA) Deriving Information on Surface conditions from Column and Vertically Resolved Observations Relevant to Air Quality (DISCOVER-AQ) – were conducted jointly in summer 2014 to study summertime ozone pollution in the Northern Colorado Front Range Metropolitan Area (NFRMA).

The NFRMA is located at an elevation of roughly 1600-1800 m, on the plains just east of the Central Rocky Mountains. The mix of diverse anthropogenic pollution sources including urban sources, power plants, large industrial sources, agricultural activities, and oil and gas extraction contribute with varying degree to the local ozone production. Project RFP # FAAA 2016000120 has been focused on characterizing the contributions of the different photochemical drivers to surface ozone in the NFRMA through analysis of the FRAPPÉ and DISCOVER-AQ data sets and accompanying modeling studies.

This final report builds upon work described in the previous reports and presents our findings on the evaluation and updates of available emission inventories and the assessment of estimated source contributions. We expect that this report will enable the CDPHE to develop emission control scenarios to address the ozone non-attainment status of the NFRMA. The results included in this report are based on analysis using the FRAPPÉ and DISCOVER-AQ observational data sets, the Sparse Matrix Operating Kernel (SMOKE) modeling system, the Community Multiscale Air Quality (CMAQ) model, the chemical boxmodel BOXMOX (an extension to the Kinetic PreProcessor (KPP) and the NASA LaRC Steady State Model. Our derived source contributions are based on a zero-out approach of the major contributing emission sectors in CMAQ. Not all analysis and results from the two Interim Reports from December 2016 and April 2017 are included in here, but only repeated or referenced as needed to support the discussed analysis and final conclusions.

The main findings from this work are the following:

- Typical summer high ozone days exhibit upslope winds during the day characterized by transport of emissions to the west and into the mountains. Often, we observed at least a partial separation between air masses originating further north (oil and gas related emissions) and further south (Denver area urban and industrial emissions); some mixing can occur, especially if the upslope winds have a northeasterly component.
- Specific meteorological conditions such as the Denver Cyclone can have a large influence on the magnitude of ozone production by more efficiently mixing VOC from oil and gas sources with NOx emissions in the urban areas. This causes a different, more local distribution of ozone, concentrated in eastern Boulder, Gilpin, and northern Jefferson counties.
- Mobile sources and oil and gas related emissions are the largest contributors to local ozone production in the NFRMA. On average, oil and gas emissions show a stronger influence in the northern part of the NFRMA and the northern foothills, while mobile

emissions dominate farther south and in the southern foothills. Both sectors contribute, on average, 30-40% each to total NFRMA ozone production on high ozone days.

- Industrial emissions contribute somewhat less to NFRMA ozone on average, but can dominate locally, as is the case in and around Commerce City.
- NOx from power plant emissions as well as from Denver International Airport causes ozone titration locally due to large NOx emissions in a confined area. Further downwind the additional NOx can result in net ozone production in the western part of the NFRMA on high ozone days, albeit over a limited area. Reduction of NOx from these sources will result in higher ozone locally and slightly lower ozone in areas further downwind.

1 WRF Meteorological Simulations and CMAQ Modeling Setup

The CMAQ modeling work is conducted using the latest CMAQ version v5.2 beta with the carbon bond mechanism version 6 (CB6r3) mechanism (we acknowledge Deborah Luecken (U.S. EPA) for providing the model version ahead of a public release and for help with running the model. WRF v3.8.1 is run to create hourly meteorological fields for driving CMAQ. In here we only provide a brief overview of the model setup, for a more detailed description we refer to Interim Report II (April 2017).

The CMAQ domain is comparable to the domains used in the Denver SIP modeling and includes a 12 km x 12 km outer domain (d01; EPA CONUS12) covering the Western U.S. and a 4 km x 4 km inner domain (d02; EPA CONUS4) over Colorado. The model top is set at 50 hPa with 37 vertical levels. We use NCAR ECMWF analysis fields (available from NCAR's Research Data (RDA), https://rda.ucar.edu/) for meteorological initial and boundary conditions and Real Time Air Quality Monitoring System (RAQMS) model output (provided by Brad Pierce, NOAA NESDIS) for chemical initial and boundary conditions.

We applied analysis and observational nudging in the WRF simulation following suggestions from the Western State Air Quality Modeling Study (WSAQS) (UNC, 2016). In brief, analysis grid nudging is applied to the outer domain (d01) with nudging for temperature and water vapor mixing ratio turned off in the boundary layer. Observation nudging was performed for the inner domain (d02) for winds, temperature and water vapor mixing ratio. For our first model simulations, we included NCEP ADP Global Upper Air and Surface Observational Weather Data available from the NCAR Research Data Archive (RDA) website in the observational nudging. Tests with adding wind, temperature and dew point observations from FRAPPÉ and DISCOVER-AQ in the observation nudging showed a small but notable improvement, which is why the latter has been used in the final runs. A discussion on the performance of model transport and meteorology is given in Section 2.

Emission inputs for CMAQ are based on a set of different inputs which are summarized in Table 1 in Interim Report II (April 2017). We acknowledge Dennis McNally (Alpine Geophysics) for providing the 2017 onroad mobile inventory data and Dale Wells (CDPHE) for providing the 2014 oil and gas (O&G) emission input data. EPA emission totals were derived from the EPA 2011 v6.3 platform (ftp://ftp.epa.gov/EmisInventory/2011v6/v3platform/reports) and the EPA 2014 Emissions Inventory System (EIS) sector summary (https://www.epa.gov/air-emissions-inventories/2014-national-emissions-inventory-nei-data ;download date: 05/04/2017). The EPA 2017 emission information is derived from the emission summary available from

ftp://ftp.epa.gov/EmisInventory/2011v6/v3platform/reports/2017ek_county_monthly_report.xlsx (download date: 03/28/2017). At the time of the study, EPA 2014 SMOKE-ready input files had not yet been available. The emission inventory derived from these inputs is defined as "a priori" or "S0" in this document.

In Table 1 we list the emission totals per county and also the county total per sector for the S0 inventory. Onroad mobile emissions account for about 1/3rd of all NFRMA anthropogenic emissions with largest contribution from the Denver counties. O&G sources amount to the second largest NOx sources with most of them attributed to Weld County. NOx from industrial sources is largest in Denver county, where Denver International Airport (DIA), which is considered an industrial source, represents a major emitter. Cherokee power plant in Adams County is the largest contributor to CEM emission followed by the Valmont power plant in Boulder county. For VOC, O&G activities, mostly in Weld County, account for about 50% of all NFRMA emissions. Industrial sources are the second largest contributor with most emissions located in the Denver counties.

Table 2 compares the a priori (S0) emission estimates for CO, NOx and VOCs to estimates from EPA 2011, 2014 and 2017. Highest emission values for all species are found in NEI 2011 as this inventory does not include more recent emission controls and cleaner technologies considered in the later inventories. S0 emissions for CO are in line with EPA 2014 and higher than in EPA 2017. For NOx, our inventory is closer to EPA 2017 than EPA 2014 which likely is due to our inventory also using mobile emissions for a 2017 projection. S0 has the lowest VOC total emissions from all four inventories with about 12% lower totals compared to EPA 2014. EPA 2017 is notably higher with similar Weld County emissions as EPA NEI 2011.

In Interim report II (April 2017; Tables 1 and 2) we compared CO, NO_x and VOC emission totals for the mobile sector and the oil and gas sector for S0 and the different EPA NEI data sets. This comparison showed that the mobile emission totals used in our study are overall lower compared to EPA 2011 and EPA 2014 and either of similar magnitude or slightly higher when compared to EPA 2017. This is also the case for the major contributing counties of Denver, Jefferson and Arapahoe. NO_x mobile emissions in our study as well as in EPA 2017 are about half of the estimates in NEI EPA 2011 and 2014 in Denver, Jefferson and Arapahoe counties, which are the counties with the highest mobile emissions. Our study totals for Weld and Larimer, in contrast, are notably higher compared to EPA 2017 and in the case of CO closer to EPA 2011 and in the case of NO_x and VOC closer to EPA 2014. For the oil and gas sector most of the contribution comes from Weld county and while Weld county totals for our study are higher in CO and NO_x compared to all other inventories, our VOC totals are lower by 39%, 17% and 37% compared to EPA 2011, EPA 2014 and EPA 2017, respectively.

Table 1: Sector emissions for NOx and VOCs for the S0 a priori emissions. Emission totals are listed per county together with the county total.

	Nox (tons/year)							VOC (tons/year)						
	Offroad	Onroad	O&G	Industrial	CEM	Others	Anthro. Total	Offroad	Onroad	O&G	Industrial	CEM	Others	Anthro. Total
Adams	1,311	4,350	1,497	1,980	5,447	53	14,639	1,163	2,391	1,173	6,498	45	532	11,802
Arapahoe	1,349	4,068	480	1,289	-	77	7,262	1,853	2,933	933	5,481	-	774	11,975
Boulder	880	2,107	24	1,591	2,067	66	6,735	1,019	1,467	233	2,710	14	683	6,126
Broomfield	121	544	3	104	-	7	779	98	336	85	636	-	73	1,229
Clear Creek	26	455	-	69	-	1	552	70	164	-	124	-	16	373
Denver	1,548	4,496	7	5,343	93	82	11,568	1,419	3,014	29	6,682	5	859	12,009
Douglas	982	2,938	-	502	-	35	4,456	998	1,588	-	2,563	-	349	5,498
Elbert	88	426	8	52	-	3	578	83	215	42	255	-	31	627
Gilpin	70	219	-	21	-	1	311	34	72	-	41	-	9	156
Jefferson	1,434	3,790	11	1,739	12	75	7,060	1,673	2,815	6	6,068	5	747	11,313
Larimer	885	4,225	21	922	1,420	69	7,542	1,305	2,341	305	3,022	38	720	7,731
Park	78	272	-	38	-	3	390	281	197	-	132	-	28	639
Weld	1,116	6,716	19,783	1,501	626	50	29,791	917	2,572	75,665	4,192	18	522	83,886
Total Result	**9,886**	**34,605**	**21,835**	**15,151**	**9,664**	**522**	**91,663**	**10,913**	**20,105**	**78,471**	**38,405**	**126**	**5,343**	**153,363**

Note: The O&G sector includes area and point sources from oil and gas exploration. Industrial combines the SMOKE other nonpoint (nonpt) and non-Integrated Planning Model (non-IPM) sector.

Table 2: Comparison of CO, NOx and VOC emissions for our a priori (SO) inventory and EPA NEI 2011, 2014 and 2017. Emission totals are listed per county together with the county total.

	Anthropogenic Emission											
	CO (tons/year)				Nox (tons/year)				VOC (tons/year)			
	EPA 2011	EPA 2014	This study	EPA 2017	EPA 2011	EPA 2014	This study	EPA 2017	EPA 2011	EPA 2014	This study	EPA 2017
Adams	64,200	55,351	52,314	49,625	23,538	17,612	14,639	14,009	16,389	12,523	11,802	16,215
Arapahoe	82,911	70,066	67,645	63,302	11,492	10,190	7,262	7,296	14,328	12,710	11,975	14,328
Boulder	43,153	35,798	35,160	33,214	8,981	8,431	6,735	6,902	9,878	6,279	6,126	8,555
Broomfield	7,550	6,615	6,578	5,403	1,347	1,297	779	822	2,019	1,326	1,229	2,019
Clear Creek	6,703	4,407	3,922	4,097	1,717	1,654	552	989	714	550	373	619
Denver	85,003	74,863	69,656	63,937	18,683	15,403	11,568	11,623	14,613	12,688	12,009	14,613
Douglas	40,635	36,085	34,690	35,741	7,297	6,876	4,456	5,089	6,804	5,677	5,498	6,565
Elbert	5,539	3,955	3,761	3,827	1,461	989	578	963	1,148	737	627	1,127
Gilpin	1,357	959	915	838	450	394	311	317	258	166	156	213
Jefferson	78,715	64,137	58,867	57,756	13,147	10,734	7,060	8,427	15,065	11,372	11,313	14,104
Larimer	55,140	40,647	48,261	38,127	10,124	7,907	7,542	6,745	23,363	7,599	7,731	9,897
Park	5,385	3,686	3,417	3,507	821	549	390	449	3,820	707	639	920
Weld	65,222	62,041	64,472	48,628	30,010	31,293	29,791	24,487	133,584	101,677	83,886	132,978
Total Result	**541,513**	**458,609**	**449,655**	**408,002**	**129,067**	**113,328**	**91,663**	**88,115**	**241,983**	**174,009**	**153,363**	**222,153**

2 Model Evaluation – Meteorology & Dynamics

For comparison of modeled wind speed and direction to C-130 aircraft observations, hourly instantaneous WRF output from the 4 km x 4 km inner domain (d02) was interpolated to the time and location of the 1-minute merged aircraft data. For comparison to surface sites, model grids containing the site location were selected and model wind speed and direction at 10 m altitude above ground level (a.g.l.) were compared to 1-hour averaged surface observations. Only data are included where both observations and model have available data.

As mentioned earlier, we apply observation nudging in the WRF/CMAQ inner domain and performed tests whether the addition of FRAPPÉ data improves the model performance of the wind fields. We included wind, temperature, and dew point observations from C-130 flights, valid P-3B aircraft wind, temperature and dew point data and available wind and temperature measurements from CDPHE sites. The evaluation with FRAPPÉ data is not completely independent as we compare in parts to the same observations the model is nudged to and have only a limited observational data set for a truly independent evaluation.

Appendix A, Figure A1 shows observed and modeled wind roses for C-130 aircraft data for the two different nudging methods, defined here as ADP nudging and ADP/FRAPPÉ nudging, respectively. The changes with ADP/FRAPPÉ nudging are small given that the FRAPPÉ data add limited temporal and spatial information and the model is only nudged to the degree that the underlying model dynamics allows. Overall, however, the addition of FRAPPÉ data improves the agreement with C-130 data. Using the wind criteria applied in our analysis of the emission evaluation (Interim Report II, Section 2.2 and Section 3 below), we find an increase in the number of matching cases for the 10-17 LT time window by about 3-5% dependent on species.

The comparison of modeled and measured wind roses is shown in Appendix A, Figure A2 for all surface sites. Note that sites not operated by CDPHE such as Longs Peak, Trail Ridge Road, NREL-Golden, Table Mountain, Platteville or Fort Collins (FC) West were not included in the nudging. In general, the changes between ADP nudging and ADP/FRAPPÉ nudging are small but noticeable. The model represents wind speeds overall well at NFRMA sites, but is too high at NREL Golden, CAMP and FC CSU and too low at RF-North, Chatfield Park, and Aurora East. ADP/FRAPPÉ nudging helps correcting for these biases. As for wind direction, we see that model results tend to have a stronger upslope component than measured at the surface sites. A possible reason for this is that the model better represents the regional picture because it does not resolve local topography or large buildings, which impact many of the NFRMA sites. This is clearly seen at RF North with the model showing the typical daytime upslope winds, while actual winds at this site are strongly influenced by nearby canyons and the proximity to the Foothills. ADP/FRAPPÉ nudging clearly improves the model performance at this site.

The local nature of the surface sites versus the more regional nature of the model is also reflected when comparing FC CSU and FC West. Both sites are close to each other, but FC CSU is located in downtown Fort Collins and likely influenced by the urban environment as wind speeds are also clearly lower compared to FC West. FC West is only little influenced by local topography or urban disturbances and reflects the regional SE upslope flow. The dominance of a more regional flow in the model is also seen when comparing La Casa and CAMP in downtown Denver. These

sites are only 3.5 km apart, but feature a quite different wind pattern in the observations, which is not resolved by the model.

In addition to grid resolution, thunderstorms might also be contributing to the stronger upslope component in the model. During FRAPPÉ, thunderstorm activity frequently interrupted flow patterns and ozone production and the forecast models tended to underpredict thunderstorms and clouds. We do not have the relevant data from FRAPPÉ available to evaluate the thunderstorm predictions in WRF/CMAQ and adding an assessment with operational radar data cannot be conducted with the provided resources. However, we compare the model to measured downwelling shortwave radiation at three surface sites (see below) which demonstrates that our WRF/CMAQ simulation also tends to underpredict clouds.

Winds for the north-eastern NFRMA are available from two sites, WC Tower and Platteville. While Weld County winds show the upslope flow in both observations and model, the Platteville measurements reveal a highly variable pattern without a dominance of upslope winds. This suggests that the local topography disturbs the flow patterns at this site, likely because it is situated in a shallow topographical depression that is not resolved in the model. The two high altitude sites Longs Peak and Trail Ridge Road, which are considered as being more representative of the free tropospheric flow regimes, show a strong component of winds from the southeast in the measurements. This is well reproduced by the model and highlights the frequently encountered upslope conditions. The model wind speed at the two mountain sites is biased high which is likely related to the sites not fully representing free tropospheric conditions due to small scale, local topography and unresolved surface roughness.

In Figure 1 we assess the performance of modeled winds, relative humidity and temperature using measurements collected from ozone sonde launches in Platteville and FC West. For the sonde data we do not filter for the time of the day, but all sonde launches took place during daytime. At Platteville, the model has challenges representing the wind direction at the lowermost altitudes and also overestimates the wind speed, similar to what has been seen in the comparison to surface wind observations. Above 0.5 km a.g.l. the model is in close agreement with measurements in representing the transition to the free tropospheric westerlies. Temperature and relative humidity are well captured in the model but the model appears biased high at higher altitudes. For FC West, we find a similar overestimate in relative humidity as for Platteville. Wind direction and wind speed, which were simulated well in the model when compared to surface sites, also show good agreement with the sonde data.

Meteorological profiles measured at BAO (Figure 2) demonstrate a good model performance for winds and temperature for both magnitude and profile shape. The relative humidity tends to be overestimated at higher altitudes in line with findings from ozone sonde launches at Platteville and FC West. There are two possible causes that could explain this bias. As will be shown in the evaluation of vertical ozone profiles and has been discussed in Interim Report II (April 2017), specifically the last week of July 2014 was characterized by enhanced free tropospheric ozone in the Front Range, which is underestimated in the model. The origin of this high ozone is not fully determined, but believed to be due to a combination of large scale transport of ozone, possibly mixed with stratospheric ozone. The higher relative humidity in the model might suggest an underrepresentation of stratospheric air. Another possible explanation might be that the model keeps more moisture in the air while in reality clouds and rain removed moisture from the air.

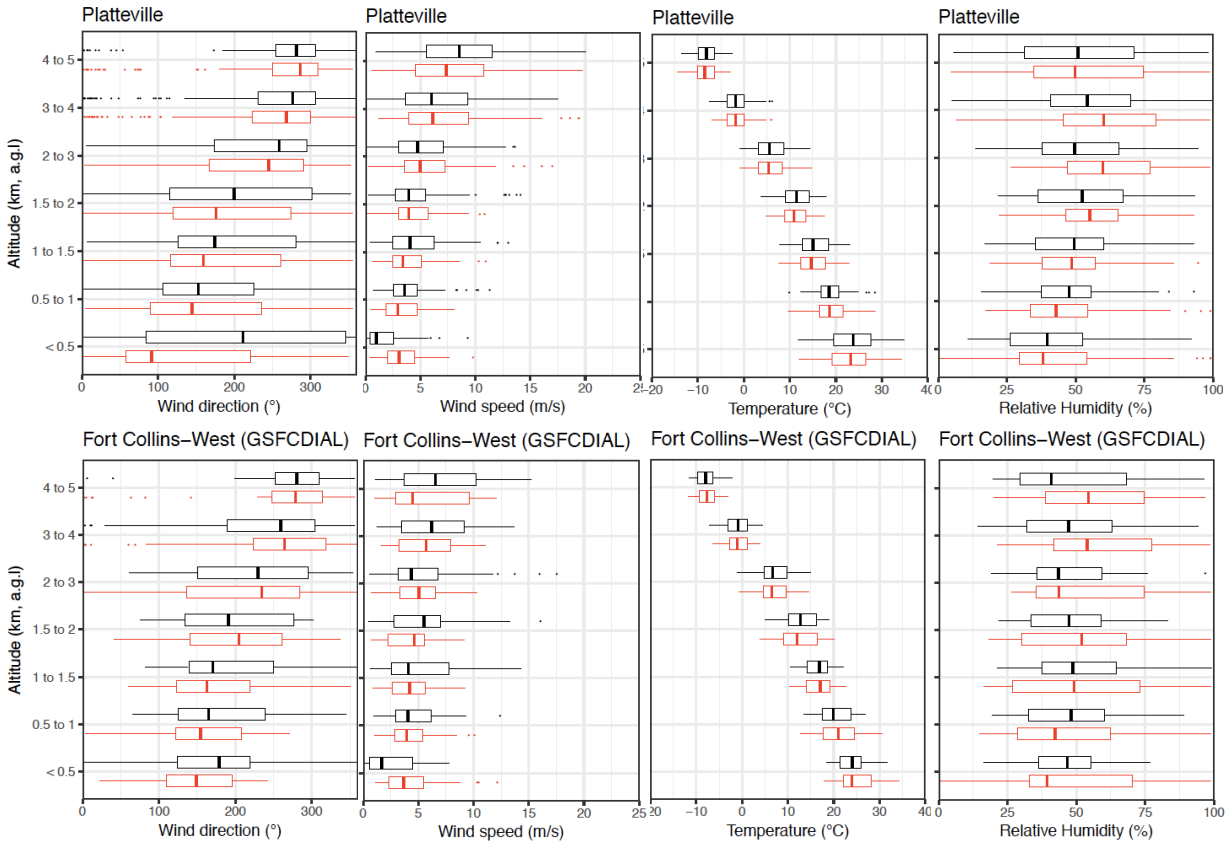

Figure 1: Vertical average profiles for measured (black) and modeled (red) wind direction and wind speed, temperature and relative humidity for ozone sonde launches in Platteville(top) and Fort Collins West (bottom).

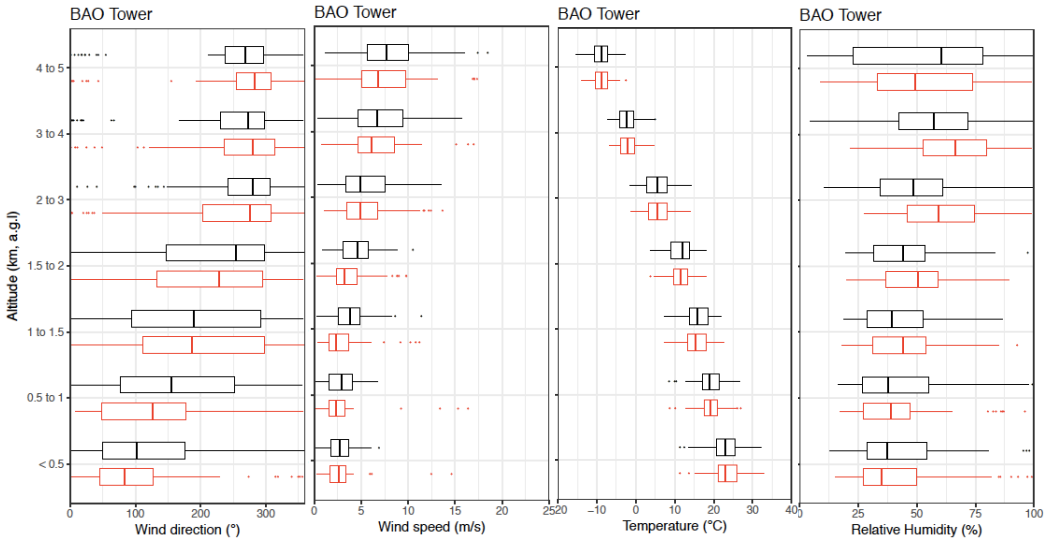

Figure 2: Vertical average profiles for measured (black) and modeled (red) wind direction and wind speed, relative humidity and temperature from the Atmospheric Emitted Radiance Interferometer (U Wisconsin) at BAO.

While the model shows reasonable performance for the wind fields, there are notable discrepancies that are related to uncertainties in the model transport, but in parts are also due to the local nature of the measurements. Overall, however, the model is able to represent the characteristics of NFRMA wind patterns and given confidence in the emission inputs, we can put trust in using the model for estimating sensitivities of surface ozone to different source types. We emphasize that our focus of the evaluation of modeled meteorology has mostly been on winds. Clearly, reasonable model representation of clouds, rain, and thunderstorms is crucial, and the comparison of the model to solar radiation measurements available for four surface sites during FRAPPÉ offers indirect evaluation of the model's ability to represent clouds.

These comparisons are shown in Figures 3 through 6 for Platteville, BAO, Table Mountain and NREL Golden, respectively. Note that for the first three sites measurements are available for 11 July – 12 August, while for NREL Golden data are only provided for 15 July-10 August. The latter site also appears to be subject to a time shift in the measurements for the first few days of the data record. This, however, does not impact the interpretation.

For BAO, Platteville and Table Mountain, which are all located north of the Denver Metro Area, there were four days with cloud-free conditions (22 July, 2&3 August and 12 August) in both the observations and the model; these days were also high ozone days and in parts are discussed later. August 2 and 3 measurements and model also show cloud-free skies at NREL Golden, but 22 July measurements indicate some clouds later in the day while the same days modeled solar radiation suggests cloud-free conditions. On most other days, the model underpredicts the amount of clouds, which has implications on the ozone production as will be discussed later. Day-to-day variability is overall similar at the four sites but localized differences are common. An example of the influence of localized cloudiness is 19 July, when measured solar radiation suggests a cloud-free day at Platteville with more clouds building towards BAO and even more clouds towards Table Mountain located further west and at NREL Golden to the south. The model does not simulate notable clouds at any of the sites for that day.

A final data set included in the evaluation of the model meteorology and dynamics is the boundary layer height (PBLH) data retrieved from Micropulse Lidar (MPL) data at FC West, Platteville and NREL Golden (Figure 7). This is not a true direct comparison, but shown here to give an indication of the model's ability to reproduce the typical PBLH and day-to-day variability. The WRF Yonsei University (YSU) boundary layer scheme is a first-order nonlocal scheme, with a countergradient term and an explicit entrainment term in the turbulence flux equation. In YSU, the PBLH is defined as the level in which minimum flux exists at the inversion level. The MPL retrieved PBLH, in contrast, have been obtained from gradients or variance in the backscatter profile, wavelet covariance, and fits to idealized profiles.

Despite the noise in the data, some unreasonable looking MPL retrievals (e.g. the first four days at Platteville), and the different definitions of PBLH, we can see that the model overall represents the day-to-day variability fairly well. Comparing PBLH amongst the three sites for the same days, it is interesting to note that the PBLH can vary notably, reflecting the local nature of sites and, in general, the variability in meteorological and dynamical conditions across the NFRMA.

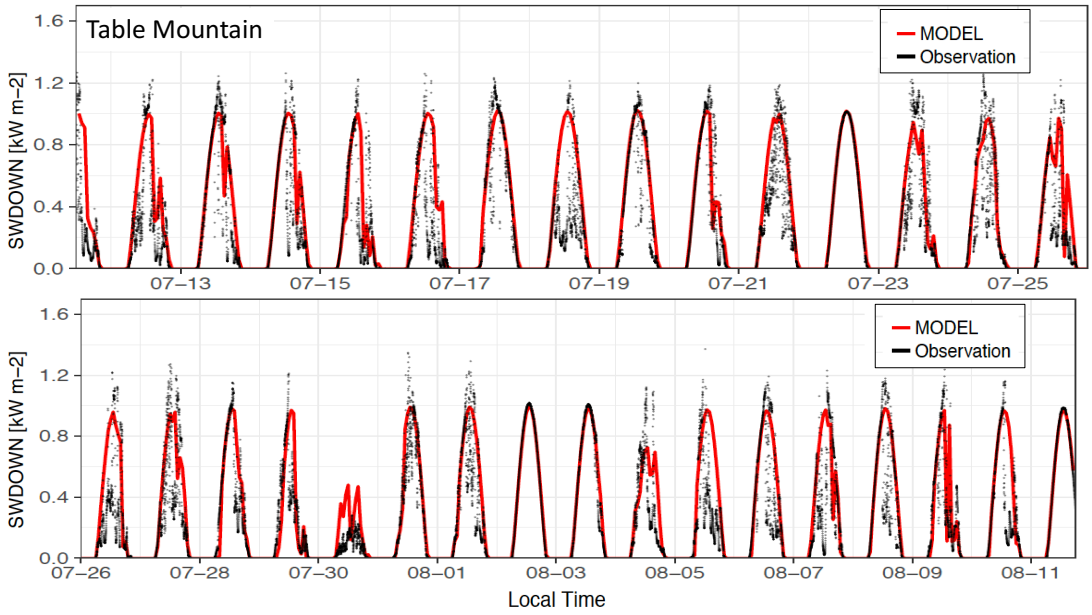

Figure 3: Time series of measured (black) and modeled (red) downwelling shortwave solar radiation at the surface for Table Mountain.

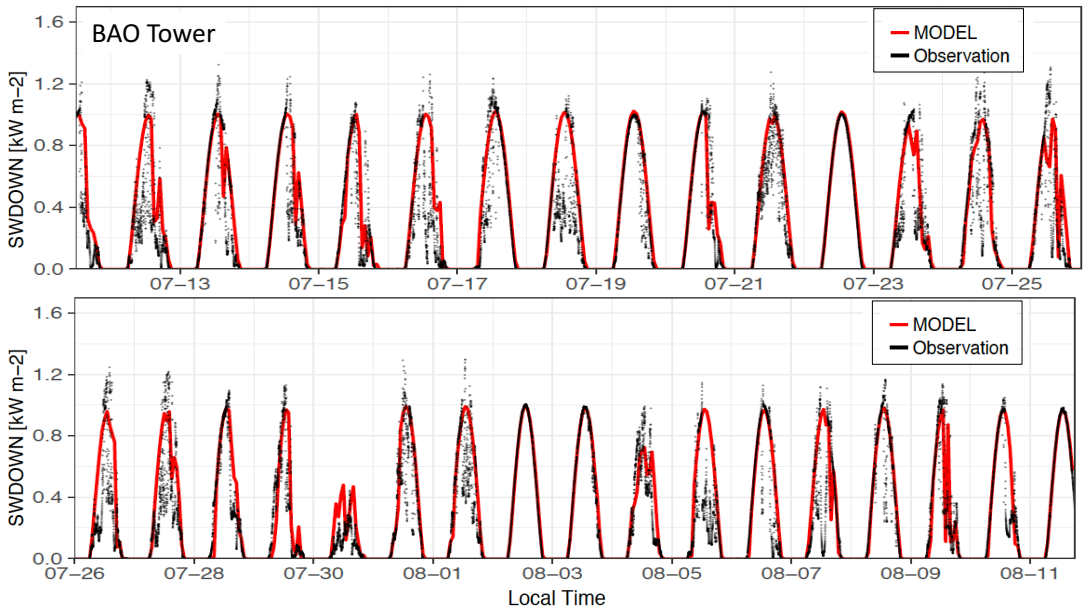

Figure 4: as Figure 3 but for BAO.

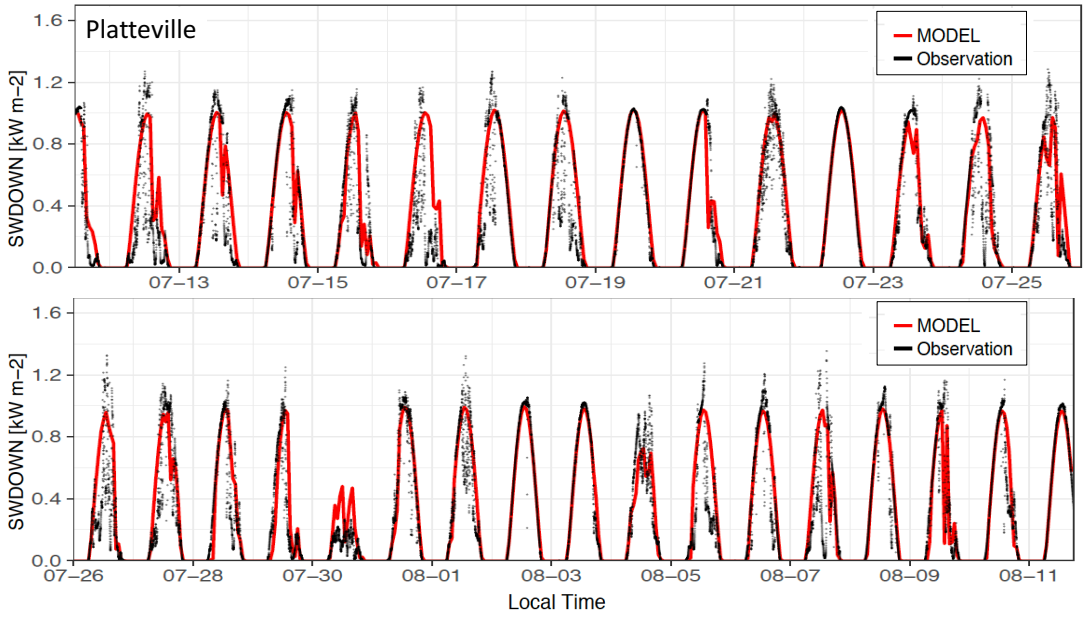

Figure 5: as Figure 3 but for Platteville.

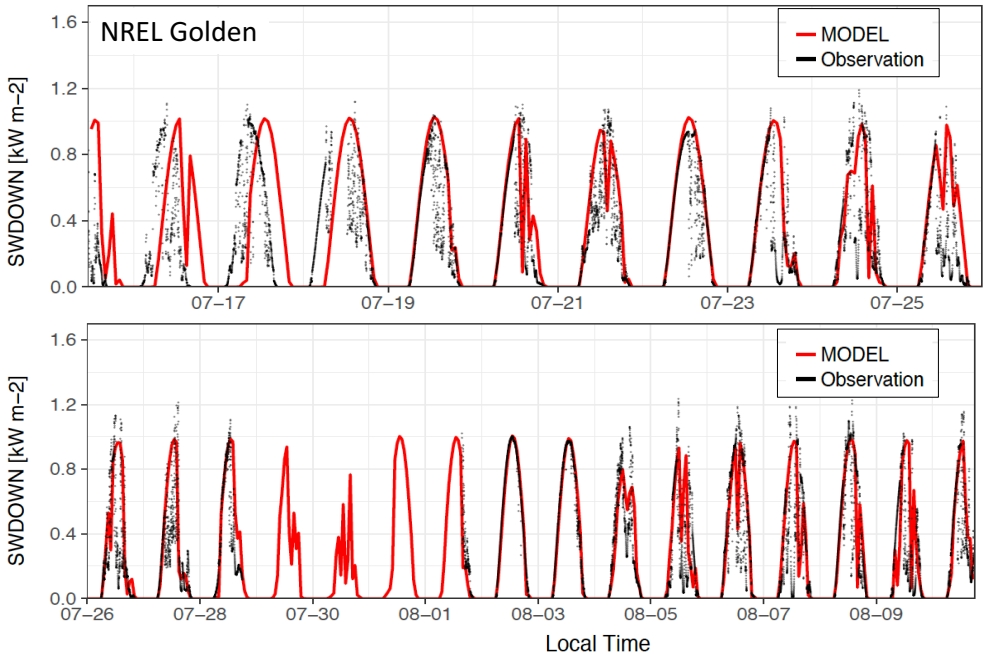

Figure 6: as Figure 3 but for NREL Golden.

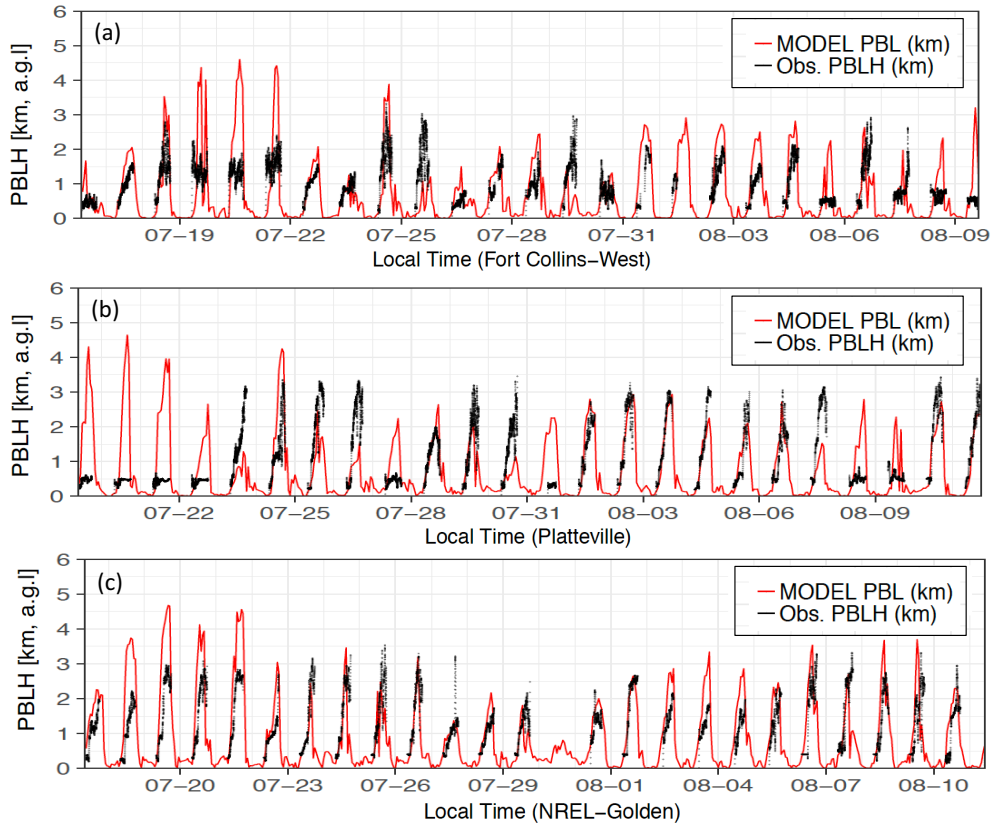

Figure 7: Time series of modeled boundary layer height (PBLH) to Micropulse Lidar (MPL) retrievals at (a) FC West, (b) Platteville and (c) NREL Golden.

3 Evaluation and Constraints of a priori NOx, CO and VOC emissions using NCAR-C130 Observations

The methodology used to evaluate the a priori (S0) emission inventory has been discussed in detail in Interim Report II (April 2017), a brief summary is given here. The base run with a priori emissions in the previous report had originally been performed with ADP observational nudging only, but has been updated to include also nudging with FRAPPÉ wind observations for this report. However, the extended observational nudging overall did not notably change the spatial or temporal distribution of trace gases or the derived conclusions.

For evaluating emissions, we focus on data from the C-130 because of its complete chemical payload. Three different regions (Figure 8) were chosen based on the dominance of certain emission sources. The Denver urban area and the non-Denver urban area are dominated by mobile emissions and, dependent on species, might also possess a large contribution from industrial emissions, whereas the oil and gas region is mostly dominated by oil and gas activities. We only filter for data where observations and modeled winds originated from within the same sector and focus on constraints in the mobile and oil and gas sector. The emission criteria are defined such that for a measurement data point to be considered, the mean emissions of not only the model grid boxes containing the actual aircraft observation but also their adjacent upwind grid boxes must have a contribution of more than 60% from either the mobile or the O&G sector.

We include only aircraft measurements for 10-17 LT and below 1 km a.g.l., which can be considered as representative of concentrations within the boundary layer (PBL) and therefore are most suited for constraining emission sources. P-3 aircraft measurements and surface measurements are used to support the conclusions derived from the analysis of C-130 data.

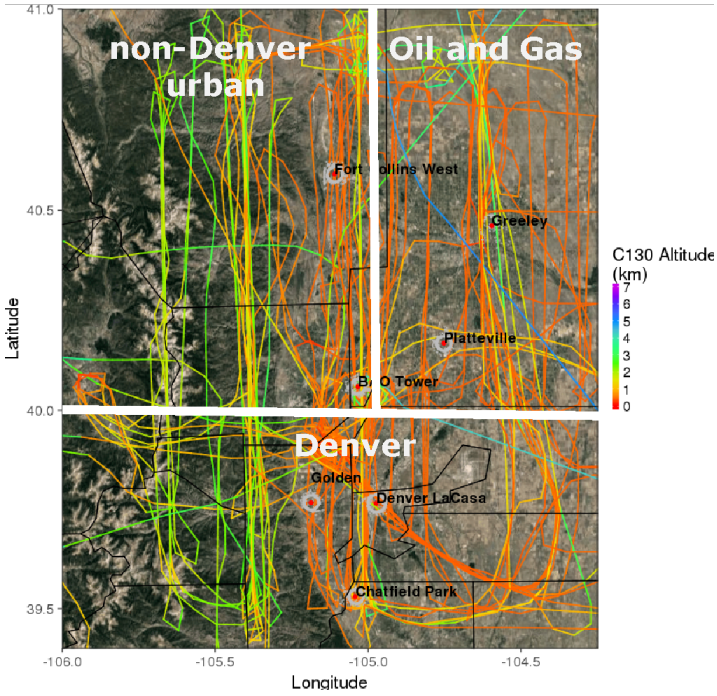

Figure 8: The three areas used for evaluating model emissions shown on a map of the NFRMA with C-130 flight tracks colored by altitude above ground level and P-3 spirals over the six key ground sites shown in grey.

In Interim Report II (April 2017) we discuss a comprehensive evaluation of the a priori (in the following referred to as S0) mobile and O&G emissions and derived the following conclusions:

- Ethyne, mostly released from mobile sources, is about a factor of 2 too low in the model while other mobile tracers and their ratios to each other are predicted fairly well by the model.
- Modeled absolute mixing ratios for the two northern subregions non-Denver urban and O&G appear underpredicted by about a factor of 2 for all mobile tracers (NO_x, CO and toluene).
- All oil and gas VOC species (alkanes and benzene) appear strongly underestimated by the model, with the exception of ethane.

Based on these results we decided to apply the following adjustments to the S0 inventory: a factor of 2 increase in all mobile ethyne emissions, a factor of 2 increase in mobile (onroad and offroad) emissions for the non-Denver urban and O&G region and a factor of 4 increase in O&G VOC emissions aside from ethane. The newly derived inventory (S1) was tested in the model; S0 and S1 model results are compared in Appendix B, Figures B1 and B2, respectively.

In order to constrain the emissions quantitatively, we show in these Figures the relationship between measured and modeled species. Only data were used that have been filtered for the agreement in wind direction and for the relative contribution of the respective emission sector as discussed above. For NOx, the agreement between S0 and S1 does not change notably as expected and because of the scatter in the comparison no clear conclusion about a possible adjustment can be derived. For the non-Denver urban region, we find a good model-measurement correlation and S1 clearly shows an improvement over S0. The model is biased

low in NOx in the O&G region, but because the mobile emissions are only a small contributor in this region, an increase in the mobile sources does not significantly change the agreement. Results for CO are similar to NOx, yet due to an instrument issue during the first part of the campaign and a smaller number of available data points only a very limited set of data is available for analysis. The increase in ethyne emissions in S1 yields to an overall better agreement for all three regions. Toluene, which also is mostly an urban tracer is now overpredicted in Denver in the model, whereas the agreement somewhat improves with S1 in both the non-Denver and O&G region, but there is still a low bias in the latter.

Benzene is released from both mobile and O&G sources and the model agrees fairly well in the Denver area in both scenarios and despite a larger scatter in the data shows an improvement in S1 over S0 for the other two regions. Ethane concentrations, which mostly originate from O&G sources, are low in the urban areas and only few data points fulfill the emission selection. Since the emissions were not changed between the S0 and S1 O&G inventories, the agreement is the same in both simulations and given the larger scatter no clear conclusion on a bias can be derived. Propane and PAR, which are unique tracers for O&G but clearly show a different characteristic than ethane, are clearly underestimated in S0 and the four times increase in the emissions brings the modeled concentrations into better agreement with the measurements.

In addition to comparing measured and modeled absolute concentrations, we also evaluate the modeled emission ratios with measured ratios. For the more typical urban trace gases we use ethyne as a reference species and for the more typical O&G trace gases we use propane as a reference species. Evaluations for S0 and S1 model runs are shown in Appendix B, Figures B3 and B4, respectively.

The ratio of NOx versus ethyne in the urban areas has a weaker correlation in the observations compared to the model which partly can be explained in that the emission criteria we apply filters for data points impacted by mobile emission in the model but because of model transport errors or inaccurate representation of the real-time traffic volume, the filtering might not be as effective for the observations. Given there are other potentially significant NOx sources in the urban areas, this will impact the analysis and might explain the discrepancy between modeled and measured ratios. While the agreement with S0 looks somewhat better, a clear conclusion cannot be drawn from the graphs. CO, in contrast, shows a tight relationship in the Denver area in both observations and model and a clear improvement in S1 over S0. Similarly, the agreement for toluene clearly improves in S1 for both the Denver and non-Denver urban regions. Benzene versus ethyne emission ratios significantly improve in S1, whereas the agreement degrades over the non-Denver urban region. The benzene to ethyne relationship in the model is similar for both the Denver and non-Denver region as a result of our filtering for mobile impacts. The ratio, however, changes in the observations reflecting uncertainties in the filtering and suggesting that this might be due to transport of benzene from O&G sources, the emissions of which were increased in S1.

For the O&G region, the ratios of NOx and CO with propane show large scatter given that both species are not uniquely emitted from O&G sources, but S1 seems to perform better for NOx whereas no clear conclusion can be drawn for CO. The increase in O&G VOC but not in ethane significantly improves the ethane to propane emission ratios in the model. Benzene versus propane and PAR versus propane ratios over the O&G region change only slightly given that all

species are increased by the same factor in S1. While the model ratios are not perfect, they are reasonably well in line with the measurements and the underlying uncertainties in the analysis (such as model transport errors that are not fully eliminated despite the filtering for wind directions, the influence of coarse model temporal and spatial resolution, incorrect boundary layer heights in the model or the limited data sampling available for the analysis which amongst other restrictions does not allow a filtering for weekends versus weekdays, inaccurate representation of realtime temporal variability in emissions, etc.) do not allow room for a further refinement of the tracer ratios.

The agreement with the C-130 observations using the S1 emissions overall improved the model performance, but in addition, we tested two other adjustments to the emissions to account for possible shortcomings found in the S1 inventory:

S2: as S1 but in order to not change the original O&G emission ratios and account for the low NOx bias in the model over the O&G region, we also increased NOx emissions from the O&G sector by a factor of 4 over a priori.

S05: as S1 but only onroad mobile emissions in the non-Denver urban and O&G region were increased by a factor of 2 and O&G NOx and VOCs were increased by a factor of 2 over S0.

Table 3 compares emission totals for the a priori S0 emissions, the first scenario S1 as well as the two additional scenarios S05 and S2. S2 has highest NOx emission totals for the NFRMA because of the increase in NOx emissions from O&G on top of the increase in mobile emissions. S05, even though compared to S1 and S2 only has increased onroad emissions versus increasing the entire mobile (offroad and onroad) sector in S1 and S2, has the second highest total NOx emissions because of the increase in O&G NOx. Offroad NOx emissions (Table 1) have been estimated to be only about 1/3rd of the onroad emissions and about ½ of the O&G emissions. VOCs did not change between S1 and S2 and totals for S05 are about half of the values for S1 and S2 and about 50% higher than S0. Changes are dominated by the different scaling of O&G emissions.

Table 3: Total anthropogenic emissions for NOx and VOCs for the a priori emissions (S0) and the four different constraints S05, S1 and S2.

	Anthropogenic Emission							
	NOx (tons/year)				**VOC (tons/year)**			
	S0	**S0.5**	**S1**	**S2**	**S0**	**S0.5**	**S1**	**S2**
Adams	14,639	14,639	14,639	14,639	11,802	11,864	11,864	11,864
Arapahoe	7,262	7,262	7,262	7,262	11,975	12,054	12,054	12,054
Boulder	6,735	8,689	9,723	9,723	6,126	7,711	8,695	8,695
Broomfield	779	888	912	912	1,229	1,306	1,324	1,324
Clear Creek	552	552	552	552	373	379	379	379
Denver	11,568	11,568	11,568	11,568	12,009	12,082	12,082	12,082
Douglas	4,456	4,456	4,456	4,456	5,498	5,498	5,498	5,498
Elbert	578	578	578	578	627	627	627	627
Gilpin	311	311	311	311	156	159	159	159
Jefferson	7,060	7,060	7,060	7,060	11,313	11,387	11,387	11,387
Larimer	7,542	11,637	12,652	12,652	7,731	10,267	11,511	11,511
Park	390	390	390	390	639	639	639	639
Weld	29,791	55,331	37,623	57,406	83,886	153,881	289,271	289,271
Total Result	**91,663**	**123,360**	**107,724**	**127,508**	**153,363**	**227,853**	**365,489**	**365,489**

Similar to what is shown in Appendix B, Figure B1 for S0, Figures B5 and B6 show the relationship between measured and modeled concentrations of the C-130 filtered data for the S2 and S05 model results, respectively. NOx in the Denver area does not change much between the different scenarios; in the non-Denver urban area the best performance is seen with S1 and in the O&G region the increase in O&G NOx in S2 leads to the best agreement. Little changes are seen for CO since the CO emissions from O&G were not increased and overall mobile emissions have a smaller contribution to CO levels. Ethyne performance is best in S1 and S2 where the emission increase is the largest. Toluene and Benzene in the Denver area change little but all three scenarios S05, S1 and S2 show a clear improvement over S0 in the other two regions. However, as mentioned earlier, even the four times increase in O&G still leads to a low model bias. This is also the case for the other O&G tracers propane and PAR over the O&G region. Ethane, because the emissions have not changed, looks similar in all model runs.

A similar conclusion can be reached from looking at the emission ratios, which are shown in Appendix B, Figures B7 and B8 for S2 and S05, respectively. Overall the best agreement is seen for S2 with the largest increase in O&G VOCs and at the same time an increase in O&G NOx. All three constrained emission inventories show an improvement over the a priori S0 emissions.

In Appendix B, Figure B9 we look now at a comparison of spatially averaged C-130 aircraft measurements to modeled values for the trace gases discussed above as well as for ozone. Only C-130 measurements below 1 km a,g,l. were used for these maps. All selected data have been averaged over a 0.1° by 0.1° grid, whereas individual 1-minute average data are included in the scatter plots. These comparisons are not filtered by the level of agreement with model winds and emission strength and model transport errors will play a more pronounced role in this comparison. However, these maps allow assessment of the ability of the model to represent the overall species distributions. We also include scatter plots of the 1-minute measurements and the model data, but there is a large scatter in these comparisons which, aside from uncertainties in model physics, transport or chemistry, is due to the model not being able to represent single measurements solely due to the coarse spatial resolution and the interpolation from hourly model output to 1-minute values.

The highest measured and modeled NOx and CO concentrations are observed and modeled in the Denver area. S2 shows the highest NOx values compared to the other model runs and also compared to observations. Interestingly, a large increase of NOx in S2 is seen in the Denver area, yet only O&G NOx emission have been increased over S1. This suggests that transport in the model towards the south is too strong on some of the flight days, which is corroborated by the highest model CO and toluene concentrations being seen south of Denver. Looking at individual flights, a large fraction of these high values is from flights on July 27 and 28 when a Denver Cyclone was established; this is also present in the model but the model does not fully represent the true spatial placement. This error in transport impacts and challenges the comparison of all species.

Toluene is overestimated in all simulations in the Denver area, but too low in the north-eastern NFRMA. Benzene is too low in S0, but appears too high in S1 and S2. For ethane, no clear bias could be determined from the previous analysis, yet this comparison seems to suggest a high ethane bias in all model runs. Other oil and gas tracers, while based on the previous analysis

appearing too low even with a four-fold increase, in this analysis seem to be simulated best in S05.

The C-130 flights over the NFRMA do not provide a comprehensive coverage in time, but were conducted on selected days dominated by either a Denver Cyclone or upslope conditions and many flights were conducted later in the day when frequent thunderstorms interrupted the transport patterns. This poses additional challenges to a model and in order to provide additional information on the performance of the different emission scenarios we discuss in Section 4 the comparison of the model to P-3 measurements and surface data.

3.1 Assessing emission constraints using P-3 and surface observations

This Section examines how well the initial emission adjustment factors derived from the C-130 observations can be reconciled with NASA P-3 and surface observations. The average spatial distribution of trace gases from the observations and the different model simulations are shown in Appendix C, Figure C1. In Figure C2 we show comparison plots for the NASA P3 spirals at the six spiraling sites as well as missed approaches at Greeley airport. We apply the same filtering criteria as for the C-130 analysis, i.e. we filter for data from 10-17 LT and below 1 km a.g.l. However, the wind filtering cannot be used because the P3 winds are not available during spirals. The spiral locations Golden, Chatfield Park and Denver La Casa are located in the Denver urban sector, the spiral sites Fort Collins West and BAO are located in the non-Denver urban area and the spiral site Platteville is located in the O&G area. The P-3 measurements represent more of the small-scale variability compared to the C130, e.g. the P-3 spirals were flown with a diameter of about 5 km, i.e. of similar order as the model grid size. The repetitive flight pattern, in exchange, allows for more robust averaging.

The evaluation with P-3 data confirms the overall conclusions derived from evaluation with C-130 data and also suggests that transport in the model towards the south is too strong. NOx overall is too high in S2 and too low in S0, in S05 and S1 the sign of the bias varies spatially. CO overall is too high independent of emission scenario suggesting a small offset in the model background value. Toluene has a high model bias in the western flight legs and spirals, but is biased low in the eastern legs and spirals. Benzene is too low over the O&G region in all simulations and overpredicted in the Denver area in S1 and S2 while S0 and S05 underpredict benzene in the Denver area. Ethane data conform the high bias in the ethane emissions as suggested from spatial analysis of C-130 data.

The spirals included in the P-3 flights provide a reasonably dense data coverage over six core sites in the NFRMA with different characteristics. For most sites ~20-30 spirals between 10-17 LT are available; over Greeley only 6 missed approaches are available. The measured and modeled vertical profiles for primary emission species for these sites are shown in Appendix C, Figure C2. Overall the conclusions derived from analysis of C-130 data and P-3 spatial distribution is replicated in this evaluation. For all sites and species, we find that during the spirals a large range of concentration values have been encountered reflecting the large variability present in the NFRMA even at single locations.

Highest NOx is measured for La Casa with the model underestimating both the median and the range. This is most likely due to the coarse model resolution not capturing the local nature of this downtown Denver site and the evaluation with surface sites discussed below will show this

further. Below we also look more closely at the low bias at NREL Golden and Chatfield. At BAO and Platteville, the best performance is seen for S05. The median and range for CO concentrations is overall fairly well captured in the model.

The comparison for toluene reflects the regionally varying bias detected during the above evaluations and overall, S05 provides the closest agreement with the observations, with toluene concentrations in the mid-range of the considered model scenarios. Benzene is highest at sites in the O&G area reflecting the large emissions from O&G sources over urban sources. S1 and S2 represent the median at BAO and Platteville best, but tend to overestimate the range. Also in the urban areas benzene tends to be underestimated, which in parts might be due to transport of too low benzene from the O&G region, but also might be due to uncertainties in the model not representing local urban sources. The range in ethane is overpredicted at most sites in the model and for BAO and Platteville the model also simulates a higher median in line with previous results. Modeled ethane at FC West is too low which might suggest incorrect transport in the model to this site during the conducted spirals but also could be a resolution issue. The concentrations encountered are on the low end.

For comparison to surface measurements of NOx, CO, benzene and toluene, which are shown in Appendix C, Figures C3 through C5, we limit the range to 9-18 LT and exclude nighttime. The PBL during nighttime is very low leading to very high concentrations. Plotting these on the same scale would make it hard to discern the daytime values from the different data sets. Because of the low PBL and the limited degree of mixing, nighttime values are also more strongly impacted by nearby sources which cannot be resolved by the model.

Surface measurements of NOx are available from 8 sites in the NFRMA with some of them also P-3 spiral sites. This allows to relate the P-3 measurements to the surface. Measurements in downtown Denver at La Casa and CAMP reflect the large small scale variability in NOx that also impacts the P-3 comparison. The two sites are close to each other and the measurements show very different characteristics with concentrations about twice as high at CAMP; model results, however, are comparable at both sites and the model has a smaller bias at La Casa. At the I-25 monitor, the model is significantly underestimating the high NOx levels, which can be expected since this site is right next to a busy interstate highway. Time series at Chatfield show a different diurnal cycle in the model compared to the observations. Model winds at Chatfield (Appendix A, Figure A2) are not capturing the north-northwest winds in the observations and likely the model does not simulate the transport correctly. Modeled NOx levels at NREL Golden are in reasonable agreement with the observations with a small low bias in all simulations.

At FC West, all model scenarios overestimate NOx and the model seems to predict the drop off in NOx about an hour earlier than seen in the observations possibly due to a too early change in wind direction from the general daytime upslope to nighttime downsloping winds. The overprediction in the model might in part be due to the selection of the model grid. For comparison with the surface data we select the model grid containing the measurement site. In the case of FC West, the site is located right at the edge of the grid box. If we compare the surface observations to a model grid cell just west of the site, modeled NOx concentrations drop by about 50%. This then would bring the higher NOx scenarios in good agreement with the observations. NOx at BAO and Platteville is predicted well by the model, except for the S2 scenario which is biased too high.

The evaluation with surface CO monitors is in parts impaired by the low measurement sensitivity of some of the sensors. Sites in Denver are subject to similar grid resolution issues as NOx but are less pronounced because of the long lifetime of CO and fewer large CO sources in the Denver area. CO at FC CSU is too low in all model simulations and the model does not replicate the relatively flat diurnal cycle in CO. Such CO behavior is not typical and indicates a local source influencing the site. A similar feature is seen at NREL Golden with all model scenarios too low compared to the measurements. CO at Platteville is well simulated in all runs. Measured and modeled values at this site approach background concentrations given that CO sources are rather small around this site.

At Platteville, we also have measurements of toluene and benzene available for comparison to the model (Appendix C, Figure C5). As discussed above, model performance of winds is poor at this site but there is a large number of O&G facilities surrounding the site and emissions from O&G reach this site independent of wind direction. For both, benzene and toluene, S05 gives the best agreement, whereas S0 is too low and S1 and S2 are too high.

The final data set we use for evaluation of the modeled emissions are canister samples with the Whole Air Sampler (WAS) that were collected from a mobile van, typically nearby larger emission sources. We note that a few locations in the WAS data file are listed incorrectly (see Section 9), but this should not bias the results notably if only tracer ratios are considered. Appendix C, Figures C6 through C9 show the evaluation for the different model scenarios. For this data set we show the comparison of emission ratios as the measurements represent strong local sources that might be too diluted in the 4 km x 4 km model resolution. We select samples that were mostly impacted by either urban sources or sources from O&G activities. To do so we filter the collected data by region, by the absolute ethane concentrations and by the i-pentane to n-pentane ratio. The thresholds that were used are indicated in the plots.

For the Denver and non-Denver urban areas, the emission scenarios S05, S1 and S2 typically show a better agreement than S0 and compare rather well with the measurements. The exception is the ratio of toluene with ethyne in the Denver area, which degrades in S05, S1 and S2, but also shows a larger variability in the samples given that industrial sources are also a major source of toluene. Samples identified as O&G samples show very high concentrations of propane, ethane and PAR. These samples were collected right next to O&G facilities and related operations such as condensate tanks, fracking fluid disposal sites, etc. The 4km model grid resolution will not be able to resolve these types of sources and some of these sources may not be part of the inventories. Even though the model values are hard to discern in the graphs, the derived slopes suggest the best agreement in S1 and S2 and the least agreement in S0. The modeled ratios of PAR to propane have not changed in the different model scenarios. The modeled slope of 3.1 is too low compared to the measured slope of 11. However, the slope derived from the C-130 data is 5.2 (Appendix B, Figure B3) suggesting that the WAS samples are influenced by the special source selection and might not be fully representative for the overall O&G emission ratios.

4 Model performance of simulated ozone concentrations

In this Section, we provide a comprehensive evaluation of the modeled ozone with measurements from aircraft, sondes and surface instrumentation. For comparison to the C-130 aircraft data we separate the flights into July and August. During July, two of the flights were conducted on days with a Denver cyclone and a slight misplacement in the modeled cyclone center can lead to large uncertainties in the species distribution. Flights in August mostly were focused on upslope flows, though the predicted upslope flows did not always materialize because of the occurrence of thunderstorms.

Appendix D, Figures D1 and D2 show the spatial measured and modeled ozone distribution for the C-130 in July and August, respectively. During July, the highest ozone values were measured north of Denver, which are generally underestimated in the model. The situation is reversed around the Denver area, where all model runs typically overestimate the measured values with S2 showing the largest bias. The model better represents the conditions during the August flights with the better agreement between measurements and model during periods of high ozone concentrations along the Foothills. S0 seems to underpredict the measurements, whereas S2 appears on the high side. P-3 measurements (Appendix D, Figure D3) show the highest ozone concentrations around the Denver area and north of Denver, which are picked up well by the model. The model tends to underpredict ozone in the eastern part of the flight paths but represents well the measured values in the western part of the flight paths, aside from S0 which appears too low in the model.

More insight into the P-3 data evaluation can be gained from the analysis of the individual spirals (Appendix D, Figure D4), which in the map graphs are only showing up as single points. At most sites the model has a low bias in ozone, which extends throughout the vertical coverage of the aircraft data suggesting an overall underestimate in background ozone. This has been discovered also in WRF-Chem simulations performed in our group (Interim Report I, December 2016) and by other members of the FRAPPÉ Science Team (Yo Yan Cui, "Using potential vorticity to specify the effect of stratosphere-troposphere exchange on the vertical distribution of ozone during the FRAPPE 2014 field campaign", presented at the May 2017 FRAPPÉ/DISCOVER-AQ Science Team Meeting). It was found that part of the low model bias is caused by the models not capturing enhanced background ozone, which is most pronounced during the last week of July. This indicates that the low model bias in ozone in comparison to the C-130 and P-3 aircraft data can in part be explained by large scale features and is not necessarily due to regional and local effects. Taking into account the low overall bias, the model agrees reasonably well with measured ozone at the lowest altitude bin and also represents the site-to-site variability. For Greeley, where only 6 missed approaches are available, the model bias is the largest. S1 and S2 simulations show the largest range, sometimes exceeding the measured range of ozone values.

Additional datasets for the evaluation of the vertical performance of the model simulations are available from ozone sonde launches at Platteville and Fort Collins West (Figure 9). For better comparison with P-3 profiles, we only show the altitude range for 0-5 km a.g.l. Modeled ozone concentrations at Platteville available from 40 ozone sonde launches are also biased low at higher altitudes, but the bias is smaller compared to the P-3 profiles and the model is in close agreement with the observations at the lowermost altitudes. Sonde profiles are available for more days compared to the P-3 flights, the latter weighted by a large number of flights towards the end

of July (6 flight days between 22 July-31 July out of 15 total days with flights). In addition, ozone data from the sondes are collected all the way to the surface whereas the aircraft is only allowed to fly as low as ~ 0.3 km a.g.l.

At Fort Collins West, twelve ozone sondes were launched. For these the model runs are too low at the lowest altitude bin except for S2, which is very close in median and quantile concentrations. The sign of the bias changes with altitude and at the highest altitude bin the models tend to overestimate the sonde measurements. This is in contrast to the Platteville sondes comparison and reflects the influence of the different launch frequency on the comparison.

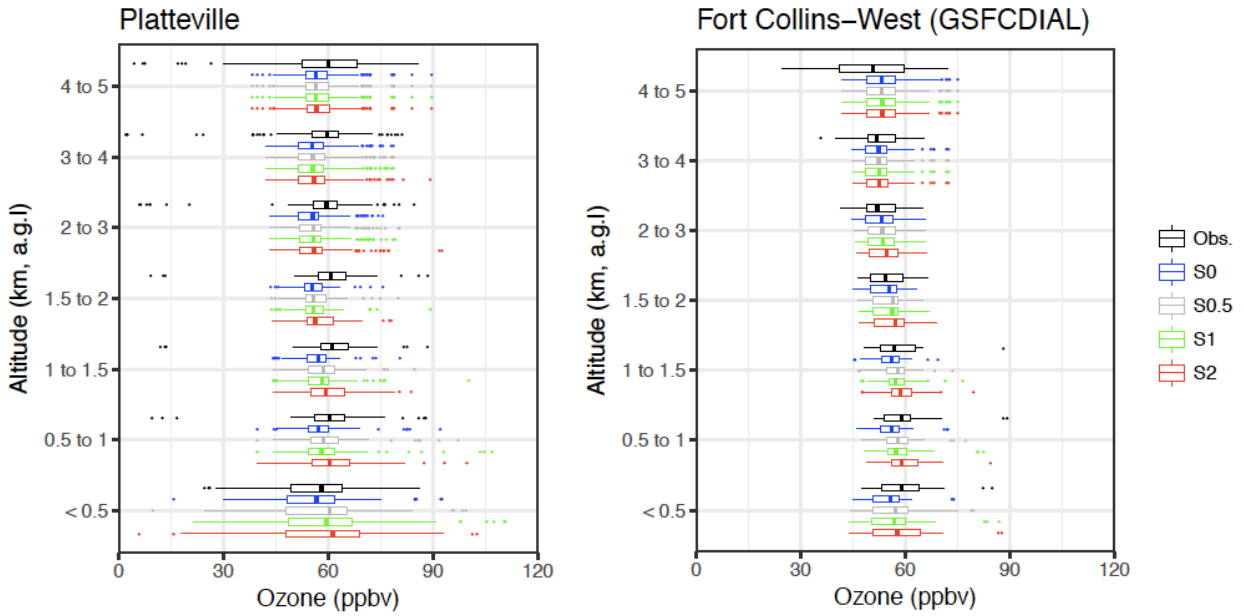

Figure 9: Vertical average profiles for measured (black) and modeled (colored) ozone for ozone sonde launches in Platteville and Fort Collins West.

Ozone measurements from tethered balloon are available at Chatfield, Fort Collins West and Denver Golf Course for 3 days each and the comparison to modeled ozone is shown in Figure 10. Tethered balloon measurements represent the near-surface vertical variability and reach up to about 0.8 km a.g.l. The launches were planned to be conducted on days with high ozone, which was not always successfully achieved. The model agrees well with the measurements at Denver Golf Course and is slightly too high at Chatfield and Fort Collins West. The model generally underestimates the variability in the measured ozone concentrations and also the vertical variability which has to be expected when comparing the model to a high-frequency small scale data set.

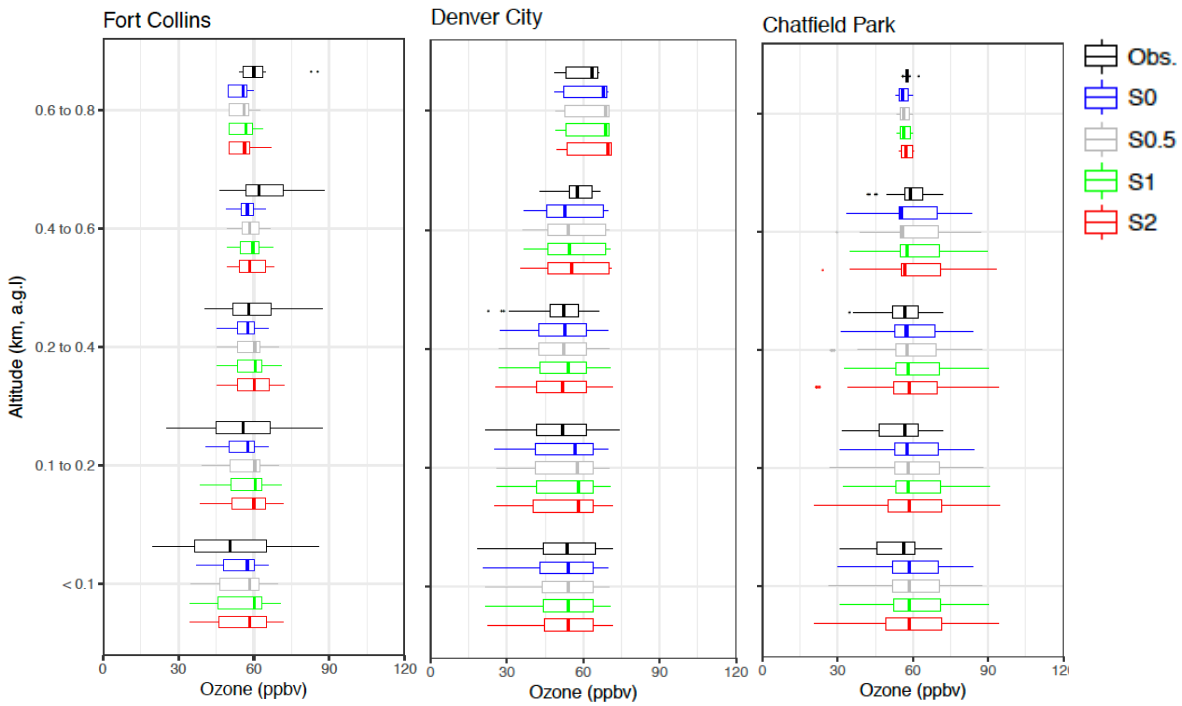

Figure 10: Vertical average profiles for measured (black) and modeled (colored) ozone for tethered balloon launches at FC West, Denver Golf Course and Chatfield Park.

The final data set explored are ozone measurements available during FRAPPÉ from 43 surface monitors (8 out of them are located outside the NFRMA or the nearby mountains but are still included for completeness). The average diurnal cycle in measured ozone compared to the different model scenarios is shown in Appendix D, Figure D5.

For most surface sites the model tends to overestimate surface ozone with S2 showing the highest ozone concentrations. A major part of this high bias might be explained by the underrepresentation of clouds in the model as was discussed in Section 2. The reverse sign of the bias when the model is compared to P-3 measurements and to a lesser degree the ozone sonde data can be explained in that flights and sonde launches were favored for days when no or little cloudiness was expected. In addition, a large fraction of the flights took place during a period of enhanced large scale background. The surface sampling, in contrast, is continuous throughout the campaign period independent of meteorological conditions. The FRAPPÉ period was characterized by above average rain and thunderstorm activity, often very localized and more likely to occur during the afternoon. For many of the sites, e.g. Chatfield, Fort Collins, RF North, Weld County Tower, Table Mountain or Welby, the morning buildup of ozone is represented better in the model compared to the afternoon, which might in part be related to this issue. The uncertainties seen in winds and NOx will also translate into uncertainties in ozone as well as the local nature of many of the sites.

Most sites in the Denver area showed a low model bias in NOx and in line with this show an overprediction of ozone. Similar to what has been seen in the comparison of NOx data, for the two downtown Denver urban sites La Casa and CAMP, the models simulate similar

concentrations at both sites, whereas ozone measured at Lasa Casa is ~5 ppb higher compared to CAMP; the latter also showed higher NOx measurements. In the non-Denver urban area, we see a similarly high model bias for sites situated inside the urban environment compared to the measurements taken in Boulder or the monitor at Fort Collins CSU. Ozone at Fort Collins West or RF North, in contrast, is fairly well captured by the model.

Ozone at Weld County tower in the O&G region is well simulated in the model. This site is located in the southern part of Greeley and with winds typically from the east and southeast during the day, it does not receive the full impact of the Greeley city emissions. BAO, also in the O&G region is rather well predicted during the day. S2 model simulations at Platteville show a narrow diurnal cycle and have the highest peak ozone of all simulations, which is related to this simulation also having the highest NOx. Note that this is in contrast to P-3 profile measurements over Platteville, where the model is biased low. At both sites, early morning ozone is overpredicted by the model. Nighttime NOx values are significantly overperdicted in the model (not shown here), which likely is related to the model not representing well the nighttime PBL, and also could explain the low model ozone in the early morning at both sites.

Additional sites had been established during FRAPPÉ in the nearby Foothills alongside Boulder Canyon (e.g. Sugarloaf, Lost Angels, Coughlin Meadows). These sites are located in a narrow canyon and we do not expect the model to be able to capture this small-scale topography. Ozone concentrations at Squaw mountain (3420 m a.s.l.) located in the Foothills West of Denver, and Mines Peak (3805 m a.s.l.), west of Squaw Mountain at an exposed high altitude location, show a late afternoon peak in ozone which is too pronounced suggesting that the model is overpredicting the intensity of upslope transport of NFRMA ozone. Note that the evaluation of surface winds also indicated a too pronounced upslope in the model. This might be related to the model not simulating the frequent thunderstorm activity or the buildup of clouds that would interrupt upslope patterns and this would also lead to a high surface ozone bias in the model.

High altitude measurements are also available from three sites near Niwot Ridge, with the Tundra Lab (TL) at the highest elevation (3739 m a.s.l.). The model best represents the average condition at TL, where also the highest ozone values have been measured (concentrations ~50 ppb without consideration of upslope influence), but overestimates the effect of upslope flow. The model simulates similar values at all sites because with the model spatial resolution the small-scale topography cannot be resolved, while ozone measured at the two lower Niwot Ridge sites (~3400 m a.s.l.) is lower compared to TL. Aside from an overall high bias, the model does simulate the occurrence of upslope events reasonably well at the lower sites.

Further to the north, ozone measurements are available from Longs Peak (2743 m a.s.l.) and Trail Ridge Road (3498 m a.s.l.). Also for these sites the effect of model resolution is evident. The comparison with Longs Peak shows similar features as for the lower Niwot Ridge sites; at Trail Ridge Road, the model is biased low throughout the day and simulates very similar concentrations as for Longs Peak. Further evaluation of the model compared to surface measurements is included in Section 8.

5 Conclusion on Emission Constraints

The above comparisons to the very comprehensive measurements available from FRAPPÉ and DISCOVER-AQ provides detailed insight into the model performance of the parameters relevant for understanding all the factors impacting ozone concentrations. A conclusive evaluation of the different emission inventories is hampered somewhat by uncertainties in the modeled transport and meteorology, and is challenged even more because of the above normal cloud and thunderstorm activity during the campaign. Periods of high ozone background ozone, the source of which is not yet fully understood, further complicate the model assessment of ozone. Model performance varies strongly from day to day and is sensitive to the spatial and temporal coverage of the observations.

Despite these complications, various conclusions can be drawn from this evaluation:

- The S0 inventory overall underestimates all relevant emission species including NOx and primary VOCs; the updated inventories S05, S1 and S2 generally show an improvement over S0.
- S2 emissions perform best in regard to VOC emissions from O&G activities
- Surface ozone is biased high in all scenarios with the largest bias in S2
- Free tropospheric ozone during flight days is, on average, too low in the model owing in large parts to the model not capturing high background ozone during the last week of July.

For an emissions inventory that can be used in a base simulation and for conducting zero-out emission scenarios our selection was made for S05. S05 in many ways shows improvements over S0 and while O&G VOCs might be on the low side in this inventory, it performs better in surface ozone compared to S2. We also decided for an increase in both NOx and VOC emissions from the O&G sector so as to not modify the underlying emission ratios and also because the NOx comparison in Weld County suggested a low model bias in NOx. We note that much of the observed overestimate of local ozone production when using the S1 and S2 scenarios in the model could be due to the underestimation of clouds, as discussed in Section 2. The exact impact of this cannot be quantified, however it might explain a major part of the overall bias given that the model shows a significantly higher fraction of clear-sky conditions compared to the measurements.

The selection of S05 as our best estimate ("base case") scenario is a rather conservative choice, particularly with respect to the VOC emissions from oil and gas related activities. Thus, in the following Sections we examine not only the S05 emissions and related zero-out scenarios, but also discuss model results from the other two scenarios, which will provide insight into the variability of impacts on Front Range ozone across the plausible range of the emission profiles considered here.

6 Zero-Out Emission Scenarios and CMAQ simulations

6.1 S0.5 base case emission scenario

Following the establishment of a best estimate for the base case emission scenario, we now explore the regional impact of different emission sectors on ozone formation by zeroing out from various sectors utilizing the CMAQ model. Table 4 lists NOx and total VOC emissions by county as well as the NFRMA totals for the S05 base case and four zero-out cases where either mobile emissions (on- and offroad; Smobile), emissions from oil and gas activities (SOG), industrial emissions (Sind) or EGU emissions (SCEM) are turned off. Zeroing out mobile emissions expectedly has large impacts on the emissions in all counties, especially on NOx, with the exception of Weld, where the largest emission impact is from oil and gas on both NOx and VOC. Industrial as well as mobile emissions have significant, and comparable, impacts on VOC emissions in all counties except Weld, and EGU emissions predictably are only important for NOx emissions in Adams, Boulder, and Larimer counties where the generation units are located. For the NFRMA overall, the largest amount of NOx comes from mobile emissions, followed by oil and gas and industry, while the largest amount of VOC emissions stem from O&G activities.

Table 4: Anthropogenic emissions for the base case S05 and the different zero-out scenarios. Emission totals are shown per county as well as the county totals.

	Anthropogenic Emission									
	NOx (tons/year)					VOC (tons/year)				
	S0.5	Smobile	SOG	SInd	SCEM	S0.5	Smobile	SOG	SInd	SCEM
Adams	14,639	8,978	14,639	12,658	9,192	11,864	8,248	11,864	5,366	11,819
Arapahoe	7,262	1,845	7,262	5,973	7,262	12,054	7,188	12,054	6,572	12,054
Boulder	8,689	3,748	8,689	7,098	6,621	7,711	3,640	7,711	5,001	7,697
Broomfield	888	114	888	784	888	1,306	795	1,306	670	1,306
Clear Creek	552	71	552	483	552	379	139	379	255	379
Denver	11,568	5,525	11,568	6,225	11,475	12,082	7,576	12,082	5,400	12,077
Douglas	4,456	537	4,456	3,954	4,456	5,498	2,912	5,498	2,935	5,498
Elbert	578	64	578	526	578	627	329	627	372	627
Gilpin	311	22	311	290	311	159	50	159	118	159
Jefferson	7,060	1,836	7,060	5,320	7,048	11,387	6,826	11,387	5,319	11,383
Larimer	11,637	2,432	11,637	10,715	10,217	10,267	4,084	10,267	7,245	10,230
Park	390	41	390	352	390	639	160	639	506	639
Weld	55,331	41,743	15,765	53,830	54,705	153,881	147,650	19,375	149,688	153,862
Total Result	**123,360**	**66,955**	**83,793**	**108,209**	**113,695**	**227,853**	**189,597**	**93,347**	**189,447**	**227,727**

CMAQ model results for zero-out scenarios across the entire NFRMA are summarized in Figures 11a-d. Shown is the difference for average MDA8 between base case simulations and zero-out simulations of the four major emission sectors over the NFRMA during the FRAPPÉ time frame. Figure 11a demonstrates that eliminating emissions from oil and gas activities would significantly lower the average MDA8 by around 6-8 ppb over the entire northeastern NFRMA with the largest impact of up to 8 ppb centered over the eastern Boulder county border. This is expected since the majority of the O&G sources are situated in the western part of Weld county and transport typically is towards the west on high ozone days. The slower reacting VOCs emitted from oil and gas activities require time to build up ozone. In addition, NOx availability increases as air masses travel towards the northern urban corridor and experience these emissions. As a result, the impact of O&G emissions on average MDA8 reaches quite far west to the Continental Divide and beyond with a simulated 2-3 ppb increase of average MDA8 attributable to O&G emissions.

The zero-out scenario for mobile emissions (Figure 11b) displays a similar impact. Due to prevalent upslope transport on high ozone days the main influence of this emission sector on average MDA8 also appears offset to the west from the main traffic corridors, and is of about the same order of magnitude as the oil and gas sector. MDA8 fractions attributable to mobile emissions are around 6 ppb in central Larimer, Boulder, and Jefferson counties with decreasing values to the west and east. Influence reaches far west beyond the Continental Divide but is strongest in Gilpin and Clear Creek counties downwind of the Denver Urban area at the southern end of the study area, while the oil and gas influence reaches furthest west in western Larimer county more to the north, including Rocky Mountain National Park. This regional separation of the influence of the two major emission sectors, caused mainly by typical summer upslope flows, creates distinctly different photochemical regimes. The southern NFRMA ozone production regime is generally more VOC limited due to dominant mobile emission sources while many areas in the northern NFRMA exhibit NOx limited ozone production due to the larger influence of O&G emissions. This finding is generally corroborated by the BOXMOX and LaRC Steady State model results discussed in Sections 7.1 and 7.2, respectively, but because of day-to-day variability and transport of air masses and because the box model does not consider clouds, there are exceptions to this finding, particularly in the downtown areas of the northern Front Range urban centers Greeley and Fort Collins.

It should be noted that emissions from oil and gas and mobile sources exhibit very different NOx/VOC ratios (higher in mobile, lower in oil and gas) which strongly influences the ozone production efficiency of either zero-out scenario. This cross-dependence needs to be considered when mitigation strategies are to be derived from the findings above. Locally, and on individual days, impacts from regulating one emission sector could be very different from the campaign average results shown in Figure 11.

Given the significant contributions of industrial emissions in almost all NFRMA counties, the comparably small impact when zeroed out on average ozone MDA8 is somewhat surprising (Figure 11c). Because of large industrial emissions of NO around Denver International Airport (DIA) as well as in Commerce City (likely the Suncor power plant), removing these emissions increases the local average MDA8 ozone in the model, presumably due to less ozone titration. Outside of the industrial areas between downtown Denver and DIA, where up to 2 ppb of average MDA8 ozone is attributable to industrial emissions, the impact of removing industrial emissions is overall very small across the NFRMA. However, the impact of industrial emissions can be more significant on individual days. Figure 12 shows a matrix of ozone MDA8 contributions from the emission sectors for three selected single days which had high ozone (28 July, 3 and 12 August; see Section 8 for additional analysis of the meteorological conditions leading to high ozone in the NFRMA and analysis of these days). 28 July is different from the August days because we observed a Denver Cyclone (DC) on that day. DC conditions tend to transport O&G emissions into the area west of Denver where NOx contributions from the other emission sectors can enhance ozone production. It can be clearly seen that on 28 July the influence of O&G emissions reaches far to the south and west and the injection of VOC from these emissions causes additional ozone production downwind of the industrial NOx sources, enhancing ozone in the SW and W sectors of the metro area by 2-4 ppb. The August days shown are upslope days with a more northeasterly component on the 3rd and a more southeasterly component on the 12th. The influence of O&G VOC emissions on ozone production extends into

western Boulder and Gilpin counties on the 3rd and far into NW Larimer County and Rocky Mountain National Park on the 12th. Ozone enhancements due to the industrial NOx sources is again 2-4 ppb on both days, but effects are more far reaching well into the mountains. Still, on all three days, mobile and oil and gas sources dominate the MDA8 ozone enhancements over the entire NFRMA.

The zero-out scenario for EGU emissions (SCEM) shows average MDA8 ozone to increase in the vicinity of the power stations (the largest being Cherokee in Commerce City and Valmont plant in central Boulder county) because of decreased ozone titration with NO (Figure 11d). Likely because the southern NFRMA already has very high average NOx values (from mobile and industrial emissions) there is, on average, no indication of ozone production downwind of the power plants attributable to their NOx output. The example high-ozone days shown in Figure 12 still show initial ozone titration because of the very large, localized NOx emissions from both power stations. However, under upslope and DC conditions, mixing with VOC emissions and dilution and loss of NOx to reactive nitrogen reservoir species results in positive contributions of around 2-4 ppb to the MDA8 on all three days further downwind of the sources. This enhances ozone in western Boulder and Gilpin counties as well as Clear Creek county on days with a northeasterly wind component.

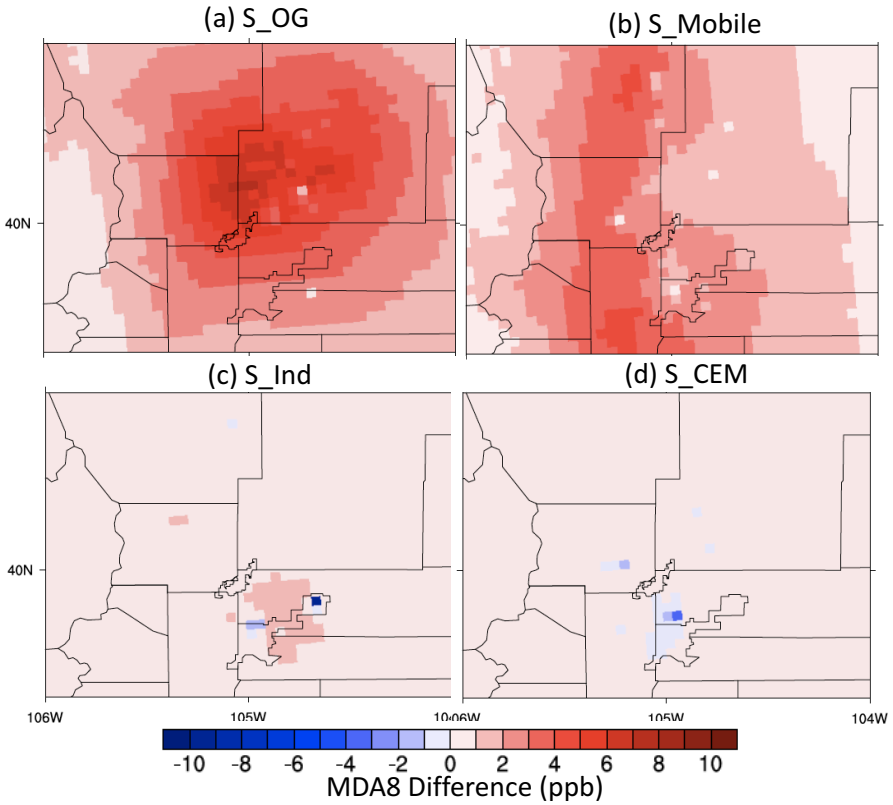

Figure 11: Contributions (represented as the difference of S05 and the zero-out scenarios) of the four main emission sectors to MDA8 averaged over the campaign period.

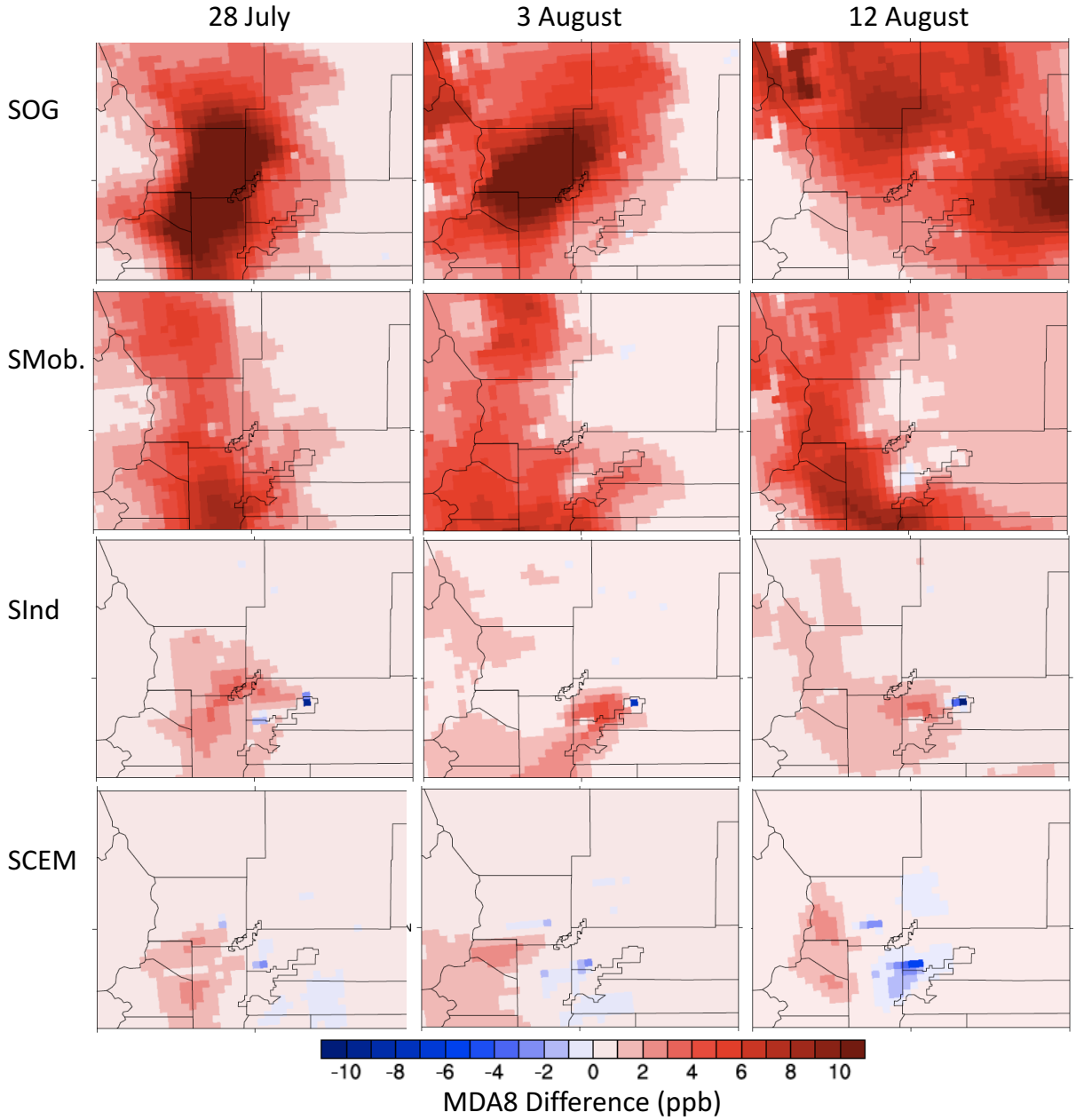

Figure 12: Contributions (represented as the difference of S05 and the zero-out scenarios) of the four main emission sectors to MDA8 on three days exhibiting high ozone values across the NFRM, as simulated by CMAQ.

In summary, the CMAQ simulations suggest that the major contributors to average MDA8 ozone values in the NFRMA are O&G and mobile emissions, with the former having a larger influence on the northern part of the NFRMA and the latter on the southern half of the region, on average. Both emission sources appear responsible for a 6-10 ppb increase in average MDA8 each, which is a very sizeable fraction of the total local ozone production over background. Figure 13 shows the difference between S05 and SBckg (all NFRMA anthropogenic emissions turned off), i.e. the MDA8 ozone enhancement in the NFRMA over large scale background ozone. Results are

shown for the average over the entire time period as well as the three selected days that were discussed above. The average enhancement is around 15 -20 ppbv, varying between 20 and 30 ppb on high ozone days with largest values typically around the larger Denver metro area; maxima reach up to 40 ppb (as seen on 28 July).

As discussed earlier, evaluation with P-3 aircraft and ozone sonde data suggests that the model underestimates the ozone background specifically in late July (Section 3.1) which could skew the average background slightly to the low side. However, while this does not linearly affect the simulated chemical ozone production, it might still introduce additional uncertainty into this analysis. The underestimate is expected to be small compared to the magnitude of the local ozone production, likely less than 1 ppb.

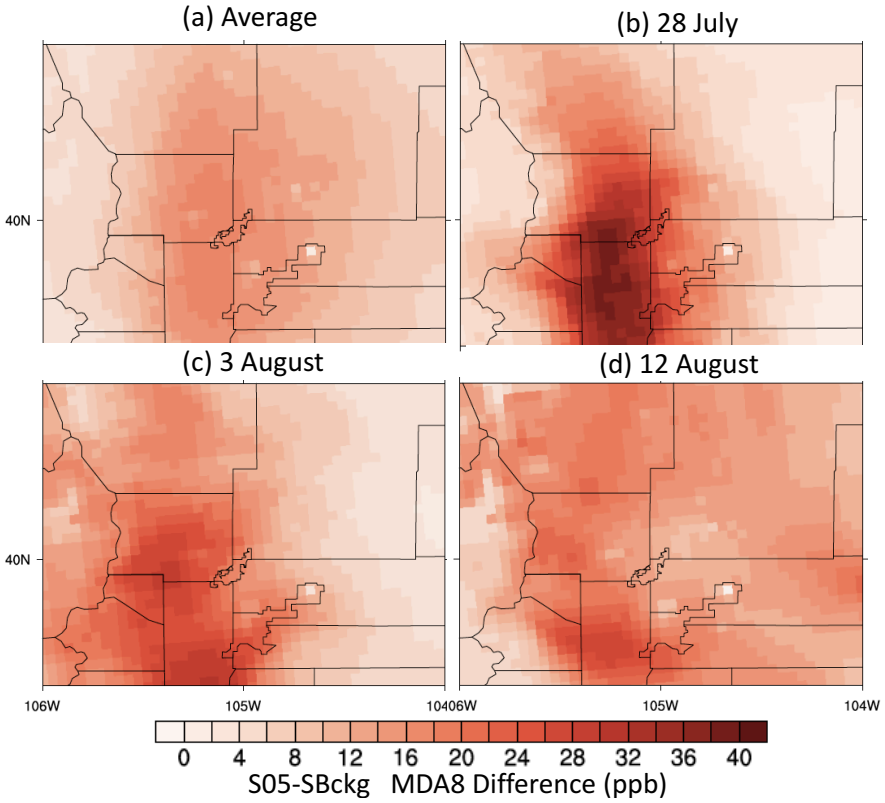

Figure 13: Difference in MDA8 ozone between S05 and SBckg for an average over the entire campaign (a), 28 July (b), 3 August (c) and 12 August (d).

6.2 Other emission scenarios

During the process of finding the best adjustment factors for the a priori emissions (S0) we developed two additional test scenarios, as described in Section 3 (Table 3). The S2 scenario differs from S05 in two ways: all oil and gas emissions (VOC and NOx) are doubled in S2 over S05 and the non-road mobile emissions in the northern sectors of the NFRMA are also doubled compared to a priori, while S05 only doubles the on road mobile emissions in the northern sectors (see Figure 8, Section 3 for details). Because in Weld and Larimer counties the contribution to NOx from non-road mobile emissions is small (12 and 3%, respectively) and

their contribution to total anthropogenic VOC is negligible in Weld county and about 15% in Larimer county, this scenario can be used as an upper limit to what would happen if oil and gas emissions again doubled in the NFRMA.

Figure 14 shows the average MDA8 ozone difference between the S2 and the base case (S2-S05) for the campaign period as well as the calculated MDA8 difference for the three high ozone days. These results show that the MDA8 ozone increase due to O&G emissions roughly scales with the emission strength for the current state of the NFRMA pollution levels. The maximum average ozone increase is up to about 5 ppb for S2 over the base case and the largest increase is located in south-central Larimer and central Boulder counties. To a lesser extent, ozone increases everywhere in the NFRMA. This is only slightly smaller than the ozone difference when oil and gas emissions are zeroed out (see above) and distributed slightly differently. The doubling in O&G NOx in S02 over S05 leads to a small decrease in surface ozone in south-western Weld County reflecting the sensitivity of ozone production to the NOx levels.

On high ozone days, the effect on the MDA8 can be much larger with an additional 10 ppb ozone formed in the western half of the NFRMA on 27 July as a result of doubled O&G emissions. On August 3 and 12 we find slightly smaller increases of the ozone MDA8 with additional ozone increases of 5 and 9 ppb, respectively, in the southwest and northwest sections of the NFRMA. On 12 August, we also see a larger increase in the south-eastern NFRMA. This is because the winds during the morning were such that they transported Weld County air to the south-east changing later to upslope flow.

These differences are closely comparable to the simulated changes in ozone when the O&G emissions are zeroed out, thus demonstrating that increased oil and gas extraction activity in the region would result in increasing regional ozone, especially in the western sections of the NFRMA, if emission regulations remained at current levels. Conversely, if the S2 scenario was to be considered closer to actual conditions, this would mean that oil and gas related emissions would be the major contributor to ozone in the entire NFRMA.

Figure 15 illustrates the difference in MDA8 ozone between the S1 and S2 scenario and thus provides keen insight into the strong dependence of the conclusions from the analysis above on the actual NOx emissions from the oil and gas sector. The two scenarios were discussed and evaluated above and both contain a fourfold increase of the a priori VOC emissions from oil and gas activities. S2 also quadruples the NOx emissions from O&G, while S1 leaves the NOx emissions unchanged from the a priori (S0) level. Section 7 discusses more in depth the photochemical regimes across the NFRMA but the northwestern NFRMA area, most impacted by oil and gas emissions, appears strongly NOx limited on average. Thus, lower NOx emissions from O&G in scenario S1 result mostly in reductions of the campaign average MDA8 ozone of ~2-3 ppb except in central Weld county (Figure 15a), where ozone in S2 is reduced by up to about 5 ppb. On the high ozone days, CMAQ simulates a further increase of ozone in western and southwestern Weld county as well as around the large NOx emitters in the Denver area on July 28 (Figure 15b). However, reduced ozone production occurs in the western sections of the NFRMA, because the ozone production efficiency drops as a result of lower NOx/VOC ratios as photochemical processing progresses downwind (Figures 15 c and d).

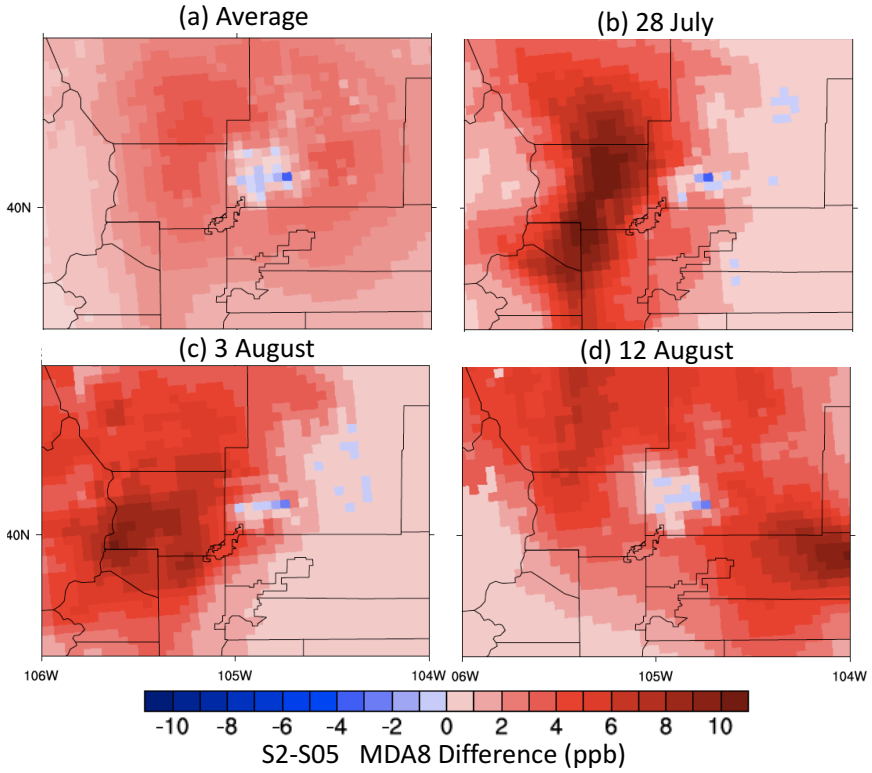

Figure 14: Difference in MDA8 ozone between S2 and S05 for an average over the entire campaign (a), 28 July (b), 3 August (c) and 12 August (d).

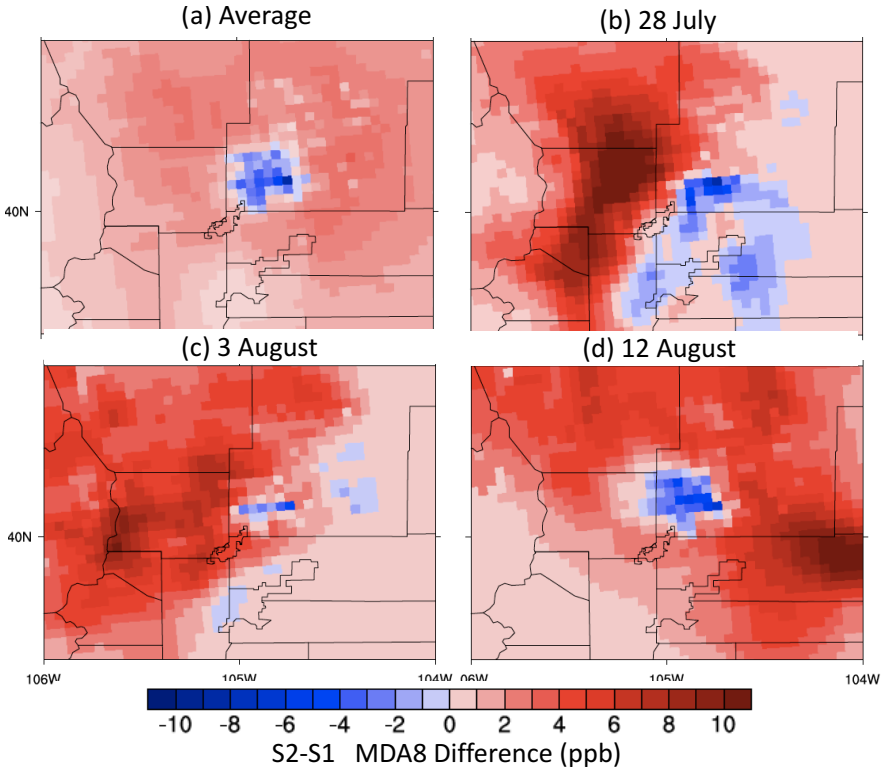

Figure 15: as Figure 14 but for the difference in MDA8 ozone between S2 and S1.

7 Chemical Boxmodeling in support of derived emission sensitivities

7.1 BOXMOX modeling

In Interim Report I (December 2016), we described the findings obtained running the BOXMOX chemical box model using C-130 observations as input to evaluate the performance of different simplified mechanisms commonly used in air quality models. Significant differences were observed between the lumped mechanisms and the Master Chemical Mechanism (MCM version 3.3), especially for some of the more reactive samples collected (i.e., over Commerce City and the Uintah Basin). We discovered that much of this discrepancy can be attributed to two issues. First, the attribution of the highly reactive aromatics in most of the lumped mechanisms is done by including these in a xylene-type species with comparably lower reactivity. Second, some of the TOGA samples exhibit what is likely a contaminant, causing very high readings of the 1,3,5- and 1,2,4-trimethylbenzenes. These very high values were the main reason for the observed discrepancies in the reactive samples that were shown.

We corrected for the contaminated TOGA samples and compared again the performance of the MOZART T1 mechanism with the MCM reference mechanism for a number of samples. Figure 16 demonstrates that the MOZART T1 mechanism compares well with the explicit mechanism for the most reactive samples collected over Denver and Commerce City after the correction to the TOGA measurements had been applied. Note that both air masses sampled are capable of producing around 40 ppb of ozone in 12 hours. Especially the Commerce City sample shows clear evidence of initial NOx suppression of ozone production. Figure 17 demonstrates that removal of the EGU emissions from the Commerce City sample would result in enhanced ozone production there, which confirms the CMAQ results above. Removal of the on-road mobile emissions from the Denver sample would result in a reduction of ozone by about 10 ppb, again confirming the results obtained with the 3D model above. Note that the removed fractions of tracers in all photochemical box model calculations are based on the S05 “base case” emission scenario.

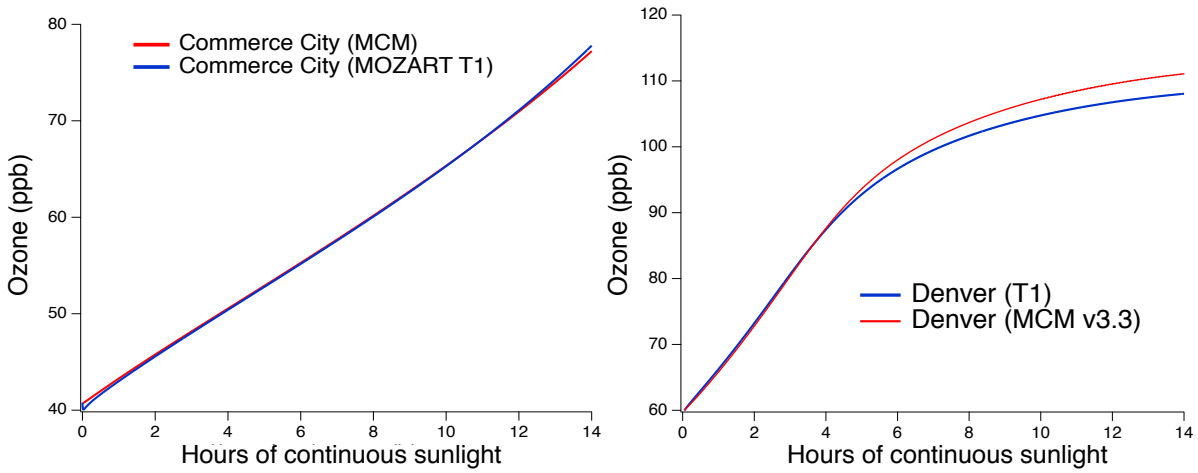

Figure 16: Comparison of ozone simulated for continuous sunlit conditions (40N, 14 LT on July 31) for the MCM (red) and the MOZART T1 (blue) mechanism. The two mechanisms agree very well for Commerce City (left), and within better than 10% for the Denver sample (right).

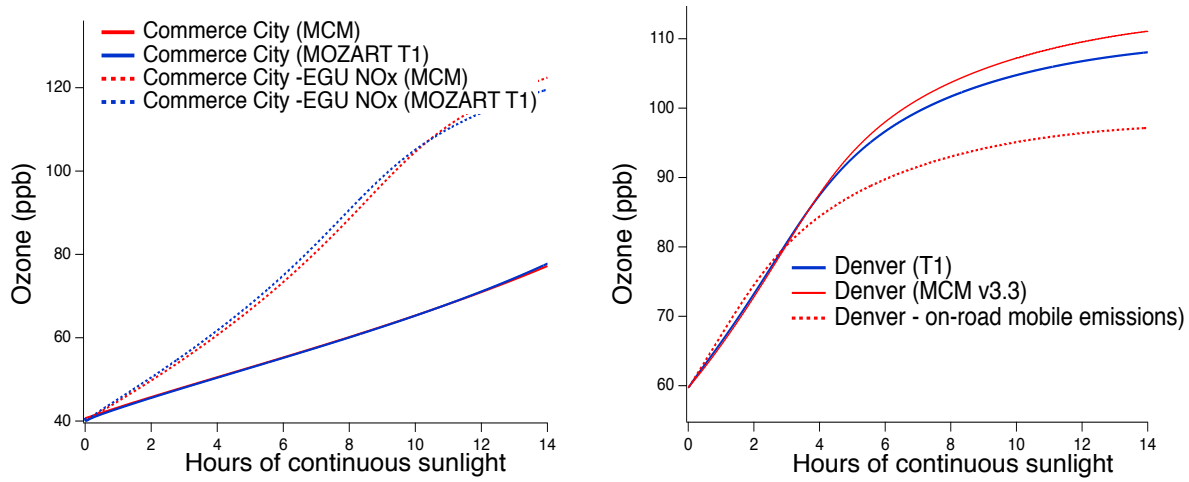

Figure 17: Comparison of ozone simulated for continuous sunlit conditions (40N, 14 LT on July 31). Like Figure 15, but with Cherokee Station emissions removed for Commerce City (left) and on road mobile emissions removed for Denver (right).

Similarly, positive results for the performance of MOZART T1 are obtained in BOXMOX with a sample collected over Weld County, and thus dominated by emissions of alkanes from oil and gas related activities (Figure 18). The MOZART T1 mechanism reproduces well the ozone production obtained with the explicit mechanism. Removal of the oil and gas related emissions is somewhat difficult in this case because the NOx emissions that can be attributed to oil and gas activities vary between 20% and 80% of the total across different areas in Weld County. In the reduced oil and gas case, added to Figure 18, the alkanes were reduced by 90% and NOx was reduced by 50% over the base case. In general, Figure 18 supports the CMAQ results, also showing very efficient ozone production over Weld County in excess of 30 ppb and a reduction of excess ozone by 30% with the oil and gas emissions removed (assuming a 50% reduction in NOx). A smaller reduction of NOx would have resulted in less reduction of ozone and vice versa, which is corroborated by the analysis of the difference between the S2 and S1 scenarios at the end of Section 6 and by results presented in Figure 15.

Due to time constraints and technical difficulties, we were not able to implement the CB6r3 mechanism into BOXMOX. CB6 is the chemical scheme used in CMAQ, but it is very difficult to integrate into BOXMOX due to its complicated allocation algorithm. We are planning to do this as soon as possible and amend the results here when they become available. However, the general speciation and species allocation of CB6 is similar to that of MOZART T1, so that we do not expect major biases in the CMAQ model due to chemistry.

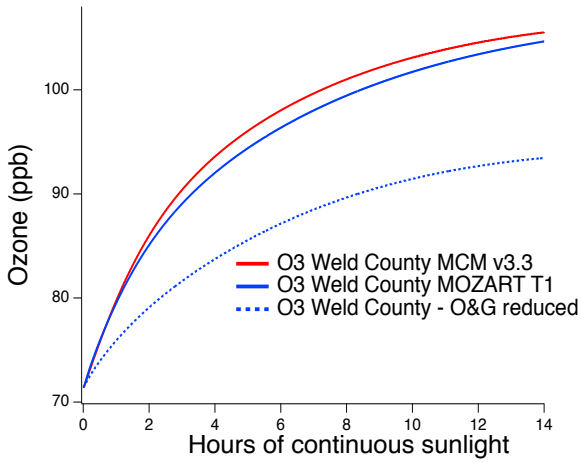

Figure 18: Comparison of ozone simulated for continuous sunlit conditions (40N, 14 LT on July 31) for the MCM (red) and the MOZART T1 (blue) mechanism for a sample collected over Weld County, and dominated by emissions from the oil and gas sector. The blue dotted lines show the change for MOZART T1 when emissions from oil and gas are removed.

7.2 NASA Langley Research Center steady-state boxmodel results

A second way of examining the chemistry and ozone formation potential of samples representative of Front Range areas with different emission profiles is the NASA LaRC Steady State Model. The model is described in Olson et al (1999 and 2006). Briefly, the model uses a diurnal steady state (DSS) approach with long- lived species constrained to measurements. In the DSS approach, each input point of in-situ data (here the data was taken from the C-130 WAS merge, and the model was run using each of the 415 canister samples for which all auxiliary data was available) is integrated by the model to find an internally self-consistent diurnal cycle for all computed species to within a given tolerance. Output is then sampled for time and date of the actual observation. The model runs were performed by Jason Schroeder from NASA LaRC and we gratefully acknowledge Jason and the Jim Crawford group for providing the results to us. The model outputs numerous parameters and steady state mixing ratios for radicals and other short lived species as well as calculated parameters. For this report, we use the calculated instantaneous ozone production rate in ppb/hr, as well as the total VOC reactivity for OH in 1/s and the ratio of peroxy radical losses via self-reaction versus reaction with NO. The latter ratio provides an indication whether the ozone production in a specific area tends to be more NOx or more VOC limited.

The areas chosen for the model runs are shown in Figure 19. They were chosen to represent both places dominated by one single source category (such as O&G in the Pawnee and NE Weld County areas) as well as mixed categories in the urban and industrial areas.

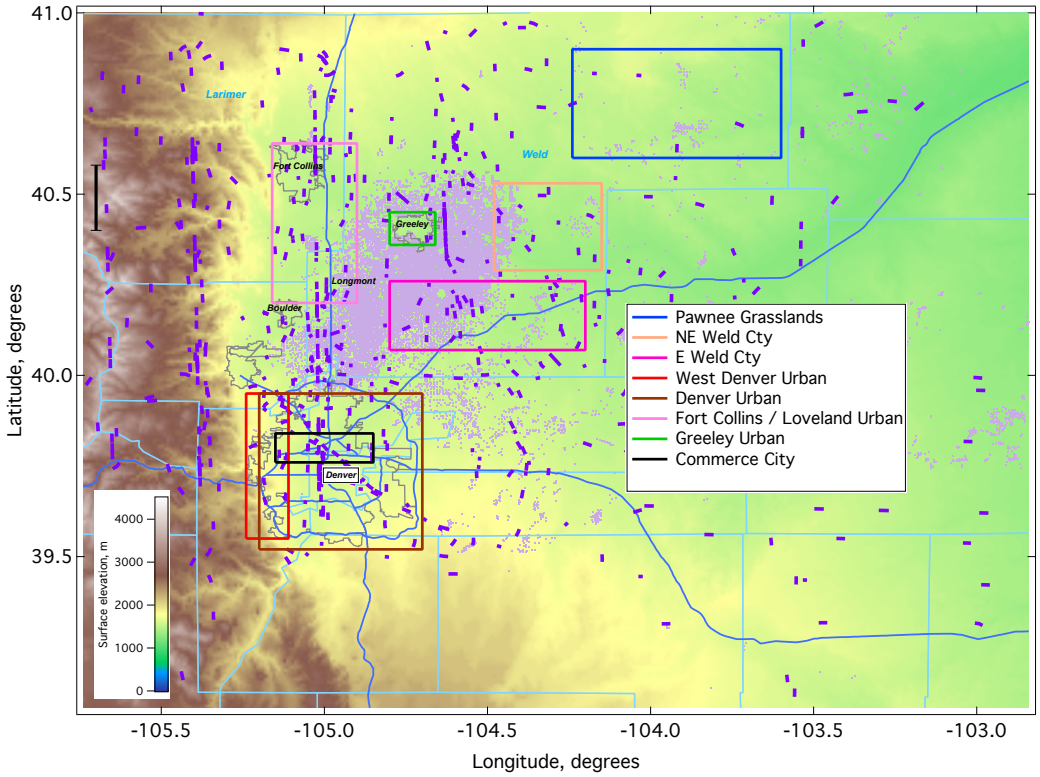

Figure 19: Areas chosen for analysis with the LaRC steady state model. The traces represent the timing for the WAS samples taken on board the C-130. Sampling time for the canisters is 10-30 seconds, depending on altitude. The steady state model was run for each sample, and runs were repeated with tracer measurements adjusted for zeroed-out emission sectors.

To examine the contributions of individual emission sectors in each area, the steady state model runs were repeated with selected emission sectors zeroed out. This was done by reducing the enhancements of individual chemical tracers over background by the fraction of each tracer attributable to the emission sector being zeroed out. The latter fractions were determined from CMAQ S05 sector emissions. Background values were obtained from WAS samples taken over the Continental Divide during westerly flow.

Several interesting conclusions can be drawn from the steady state model analysis shown in Figures 20 and 21. Note that the shown Bar-Whisker Plots include the 10th and 90th percentile and not the quantiles; mean values are indicated by the square symbol. Not surprisingly, the more remote areas that are largely impacted by oil and gas emissions (i.e., NE- and E Weld counties) show both relatively high OH reactivity and ozone production rates around 10 ppb/hr (Figure 20). Both regions are strongly NOx limited (LROx/LNOx > ~0.5 is NOx limited, LROx/LNOx < ~0.3 indicates more strongly VOC limited conditions), which also is not surprising given the large hydrocarbon emissions from oil and gas activities. Pawnee, which is the most remote area with lower density oil and gas activities, shows lower values for PO3 and OH reactivity and even more strong NOx limitation.

Greeley and Fort Collins stand out as transition areas which are under the influence of both oil and gas related emissions and transportation emissions. This causes the ozone production there to

be still NOx limited but very efficient with values over 15 ppb/hr in Greeley. Greeley displays a VOC mix that is typical for oil and gas emissions but also high NOx, presumably from mixing with local mobile emissions. This is corroborated by the zero-out scenarios shown in Figure 20, where the removal of oil and gas and on road mobile emissions by themselves lowers ozone production rates by only about 20% each.

The Fort Collins / Loveland urban (FCLove) area is more dominated by emissions from on road mobile sources, but the strongly NOx limited ozone production indicates that transport from oil and gas areas is also important. Increased NOx emissions from additional traffic expected for the future would likely, on average, increase ozone in the summer in this area.

The above results strongly corroborate the the CMAQ model results showing a fairly large influence from oil and gas related emissions in Weld County as well as the Ft. Collins/Loveland urban corridor (Section 7). In addition, the ozone monitors in the area indicate additional ozone production during transport between the monitor at CSU near downtown Fort Collins and the second monitor at Ft. Collins West (Appendix D, Figure D5).

The Denver urban area is clearly separated from the other areas by larger NOx availability as demonstrated in Figure 20. In fact, the ozone production over the Commerce City (CommCity) area is, on average, VOC limited and so is the Denver Urban (DenAM) area in the mornings. We started many C-130 research flights with a leg across Denver within the PBL immediately after takeoff and these samples have been separated from the afternoon Denver samples mainly for two reasons. First because the average sample timing in most areas matches better with the Denver area when the morning cross-city runs are removed from the average, and second because this is one chance to gain insight in how the ozone production conditions evolve over the course of the day. Despite the large NOx abundance, Commerce City and DenAM (samples taken in the Denver area during morning) still show the largest ozone production rates in the urban area. Zero out scenarios for the CEM sector were not run in the LaRC steady state model but expected NOx reductions from conversion of the remaining boilers of the Cherokee EGU will likely increase ozone in this area as strongly corroborated by both the CMAQ EGU zero-out scenario as well as the BOXMOX model runs for the Commerce City sample. The DenPM (samples taken in the Denver area during afternoon) samples show reduced ozone production rates by about a factor of 2 compared to mornings, likely caused by dilution with cleaner air originating either from above the PBL or transported in from the east. The zero-out scenarios (Figure 21) show that ozone production in both CommCity and DenAM are dominated by industrial emissions (large contributions likely from the SunCor refinery, being one of the largest source of reactive VOC in the area). These emissions likely accumulate at night and dominate Denver until dilution and continuing traffic emissions make mobile emissions the largest contributor in the Denver urban area in the afternoon, while Commerce City remains dominated by industrial emissions throughout the day.

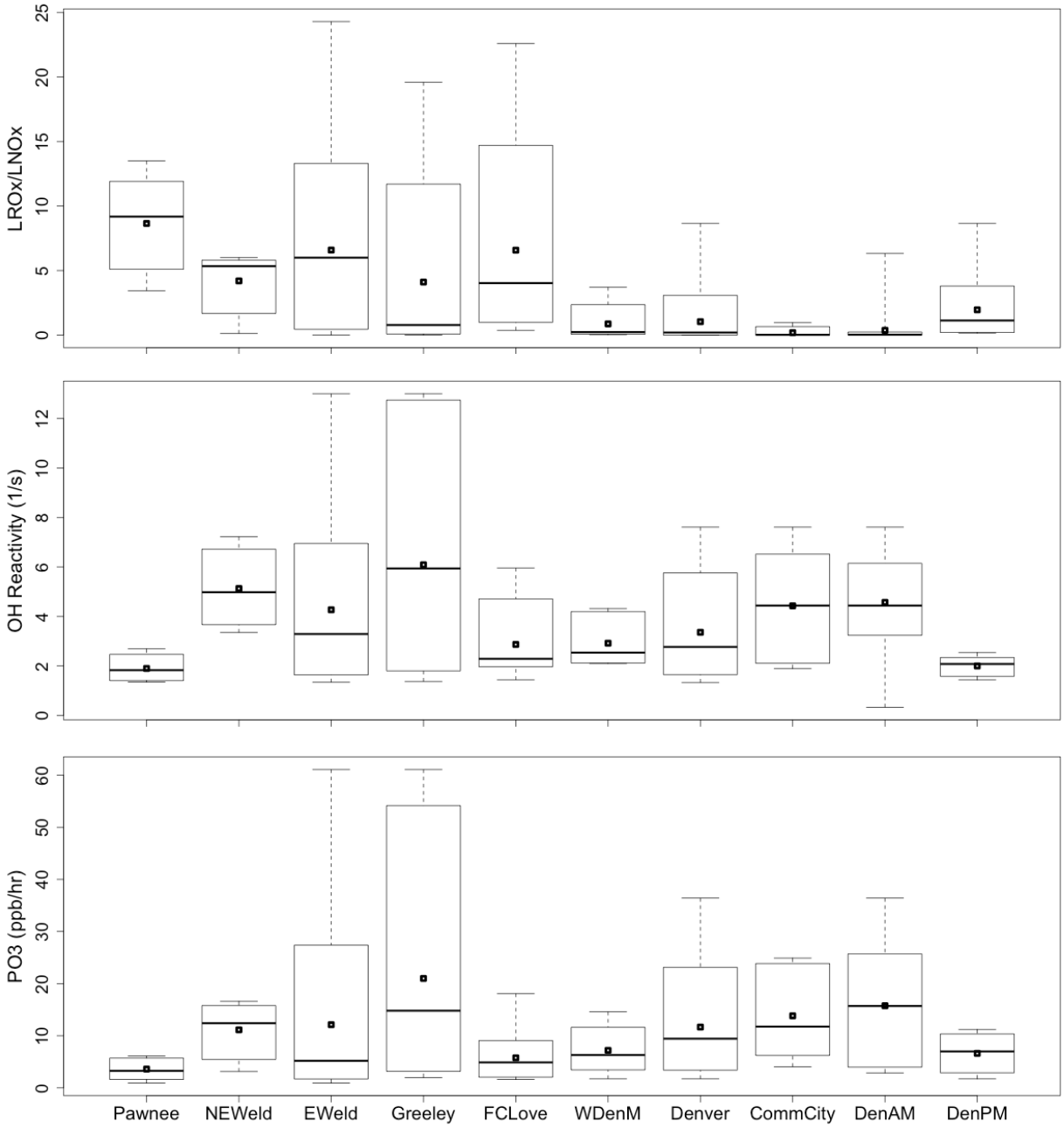

Figure 20: LaRC steady state model results for the ten areas described above. To illustrate the dependence on the time of day we show the results for Denver Urban split up into AM and PM observations. Shown are instantaneous ozone production in ppb/hr (bottom panel), total OH reactivity in 1/s (center panel) and the ratio of radical losses via self-reaction or reaction with (top panel).

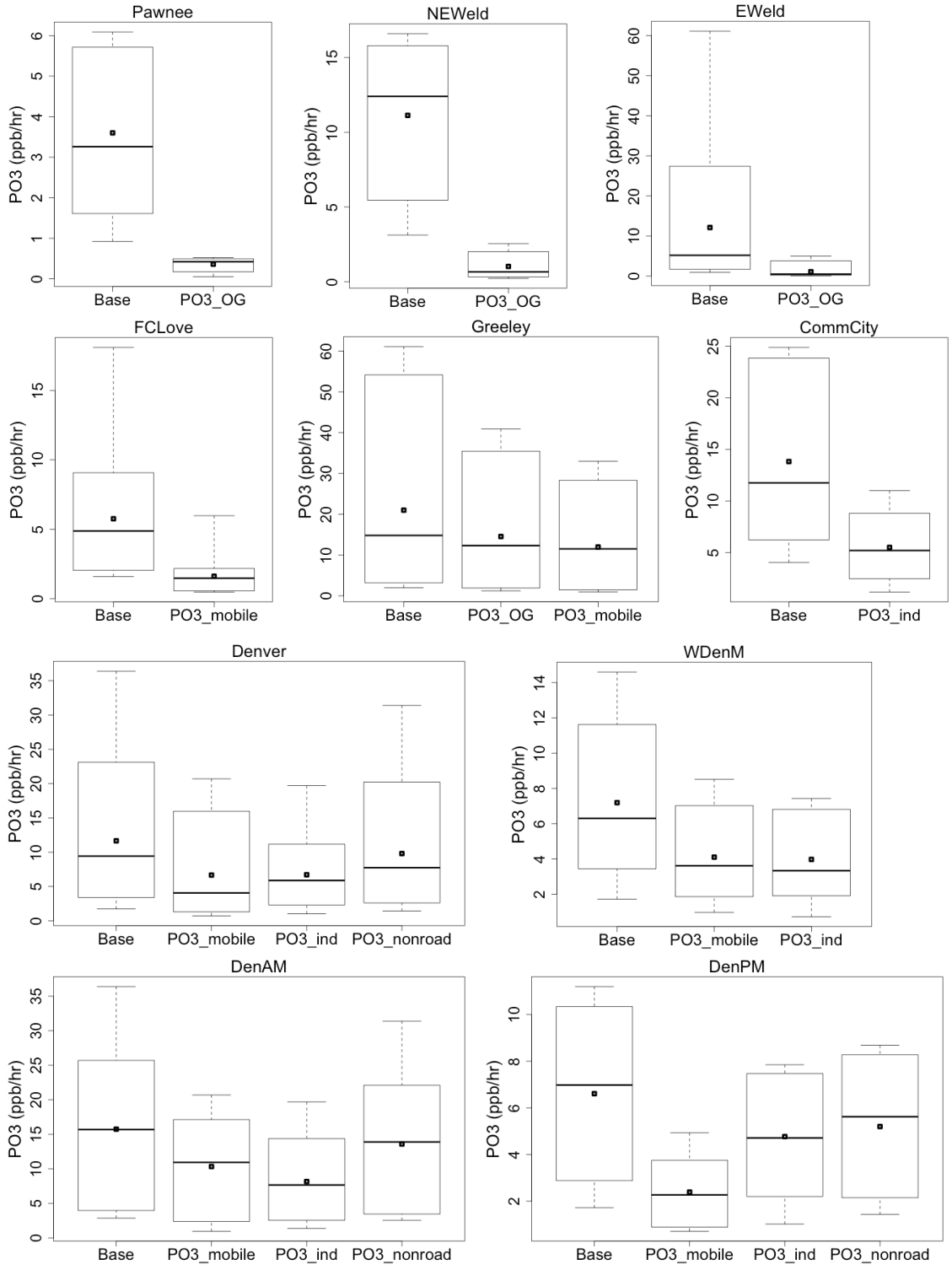

Figure 21: Ozone production rates as calculated with the LaRC steady state model for each region. Shown is the base case for each sample as well as selected scenarios where individual sectors were zeroed out (see text for more information).

8 Meteorological Patterns on High and Low Ozone Days

In the summer months, particularly during weak synoptic conditions, the local meteorology in the NFRMA is mainly controlled by thermally driven, terrain-induced, diurnal flow patterns, often also referred to as upslope/downslope or mountain-valley winds (Johnson and Toth, 1982; Toth and Johnson, 1985, and references therein). This has unique consequences for the transport, mixing and photochemical processing of local emissions (Haagenson, 1978; Greenland, 1980; Doran, 1996; Baumann et al., 1997; Olson et al., 1997) including the potential of bringing NFRMA pollution into the pristine mountains (Parrish et al., 1986; Brodin et al., 2010; Brodin et al., 2011; Benedict et al., 2011; Darrouzet-Nardi et al. 2012). Conversely, stronger frontal passages can induce outflow of NFRMA pollution to the east, impacting downwind agricultural areas in the central Great Plains. Such export events, as well as thunderstorms, are the major mechanisms for cleaning out accumulated pollution in the NFRMA.

To assess how important mountain-valley winds are on high ozone days, we show in Figures 22-24 pollution roses for measured and modeled ozone for Longs Peak and Trail Ridge Road. The data are separated into high and low ozone days, which have been defined as the average ozone concentration at either FC West, RF-North or NREL Golden for 12-18LT being > 70 ppb (high) or < 60 ppb (low). The day selection is done separately for observations and model since we are not evaluating the model for representing the actual conditions on a given day, but for its ability to represent flow regimes on high ozone days. The results are similar if other nearby Front Range Foothills sites are used or if we choose a different threshold for high ozone such as 75 ppb.

Note that there are more data points in the observations for low ozone days compared to high ozone days, which is due to the FRAPPÉ/DAQ time period overall being characterized by few high pollution episodes. In the model, this is not necessarily the case which is due to the overall high bias compared to surface ozone sites (Section 4). At FC West, we calculate 21 low and 5 high ozone days from the observations compared to 19 low ozone and 4 high ozone days from S05, respectively. The number of low and high ozone days amount to 14 and 6 days at RF North in the observations and to 10 and 12 days in the model. For NREL Golden the respective numbers of high and low ozone days is 17 days versus 3 days in the observations and 6 versus 15 in the model. The large number of high ozone days at NREL Golden is caused by the high bias in surface ozone in S05 at this site.

Figures 22-24 show that high surface ozone at the Foothills sites, in general, results in high ozone at the mountain sites. Ozone pollution roses at Longs Peak and Trail Ridge Road are shown for 12-20LT to accommodate that the highest ozone concentrations at mountain sites are typically reached late afternoon/evening. On high ozone days, the measurements show a strong component of upslope flows with elevated ozone concentrations (> 60 ppb) during the afternoon, whereas for low ozone days the dominant wind direction is from the west and northeast with ozone concentrations mostly below 60 ppb. This is in line with findings by Reddy and Pfister (2016) who state that high ozone days occur mostly on days with upper level high pressure ridges. In addition to bringing warmer temperatures and fewer clouds, upper level ridges in this region reduce synoptic winds and thus allow cyclic terrain-driven circulations. It is interesting to note that at Longs Peak the dominant wind direction on FC West high ozone days is from the SE compared to the S-SSE for the other two sites.

The model reflects the measured wind statistics well and on high ozone days suggests significantly enhanced ozone from the southeast sector. Longs Peak shows a higher variability of the measured wind direction compared to Trail Ridge Road and the modeled winds at Longs Peak are from the southeast, similar to measured and modeled winds at Trail Ridge Road, whereas the observed winds are from the south-southeast. This is explained by the Longs Peak sites being located in the valley of Cub Creek, which has a northwest to southeast orientation and likely channels the local winds, whereas the site of Trail Ridge Road is more exposed and somewhat better captures the regional flow.

In Figure 25 we provide examples of four selected days on which both observations and model show elevated ozone concentrations in the NFRMA. A common feature on all days is a general upslope direction even though the exact direction of the upslope flow can vary and locally there still might occur disturbances in the flow pattern. On all selected days, we find enhanced ozone at least at one of the high elevation sites located west of the NFRMA.

Another meteorological feature that can lead to high ozone concentrations includes the Denver Cyclone. A Denver Cyclone forms when a low-level moist, southeasterly flowing air mass meets the Palmer Divide. If the moist air lifts over the ridge and meets northwesterly winds originating in the Rocky Mountain foothills, winds may converge to create enhanced cyclonic vorticity. Dependent on the location of the center of the Cyclone, different types of emissions are injected into the cyclone and mixed within this flow leading to efficient ozone production. During the campaign, Denver Cyclone conditions were experienced on two days: July 27 and July 28. Measured and modeled surface ozone and winds for these days are shown in Figure 26. While the model represents cyclonic conditions on both days, it incorrectly places the Denver Cyclone on July 27 too far south misrepresenting the area of high ozone. The distribution on July 28 is represented better showing the highest ozone in both model and observations in and at the edge of the Cyclone.

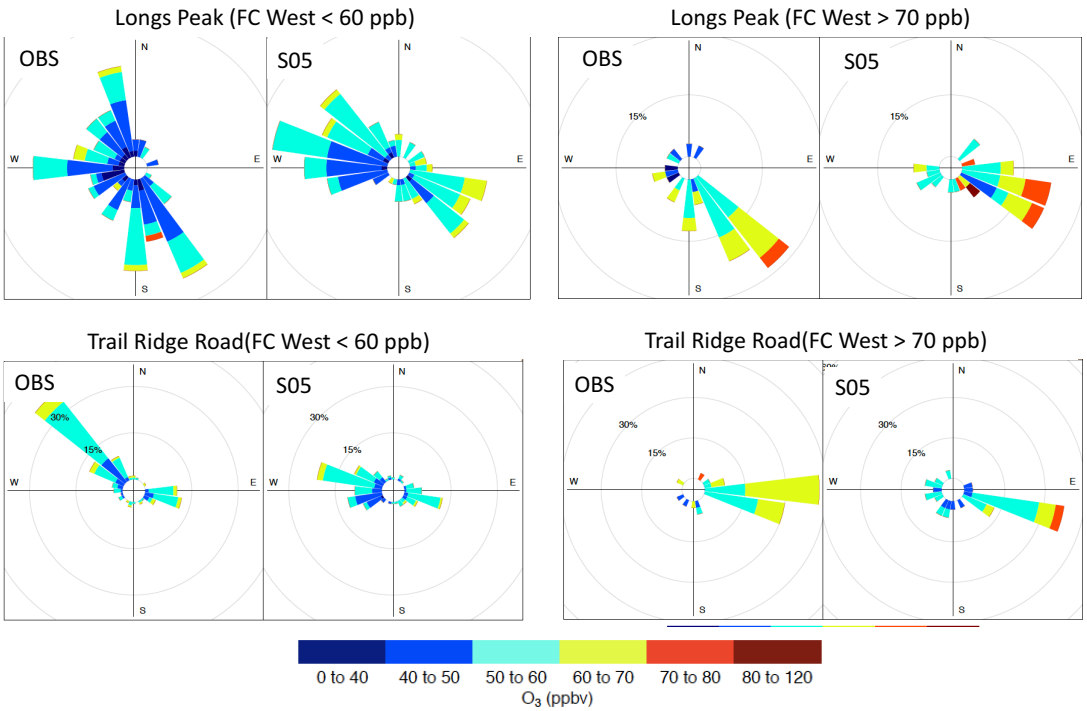

Figure 22: Measured and modeled ozone pollution roses for 12-20 LT for Longs Peak (top) and Trail Ridge Road (bottom) for days when FC West mean afternoon ozone was < 60 ppb (left columns) or > 70 ppb (right columns).

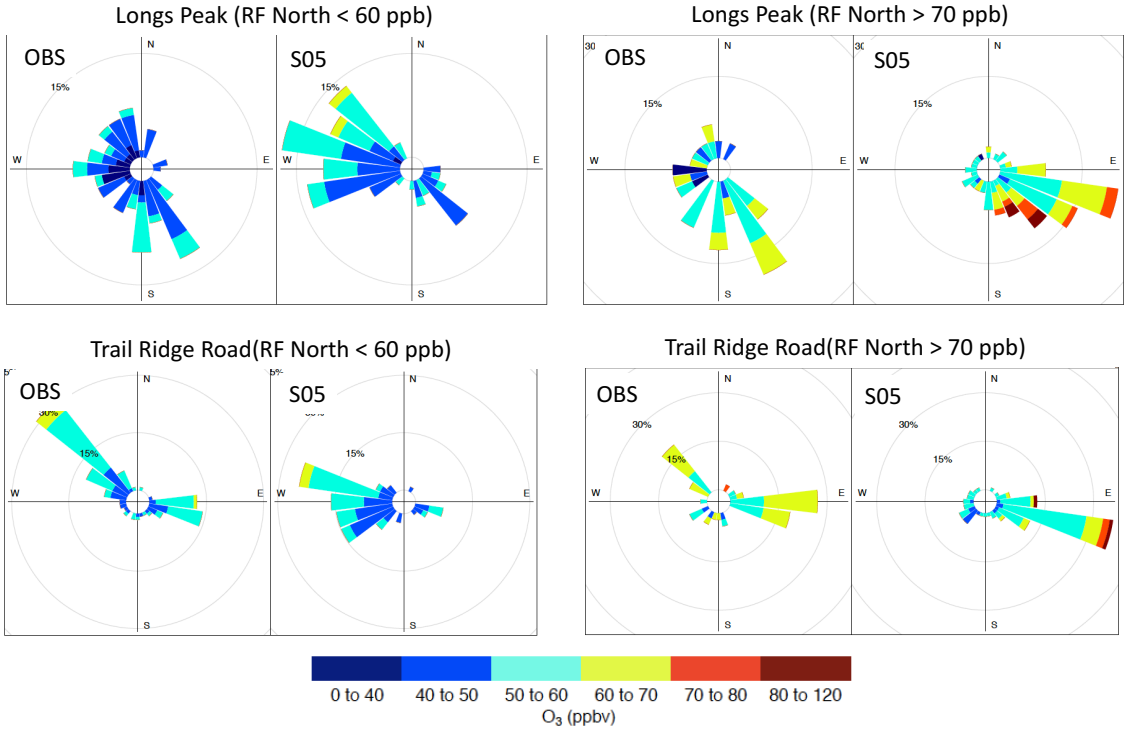

Figure 23: as Figure 22 but for days when RF North mean surface afternoon ozone was < 60 ppb (left columns) or < 70 ppb (right columns)

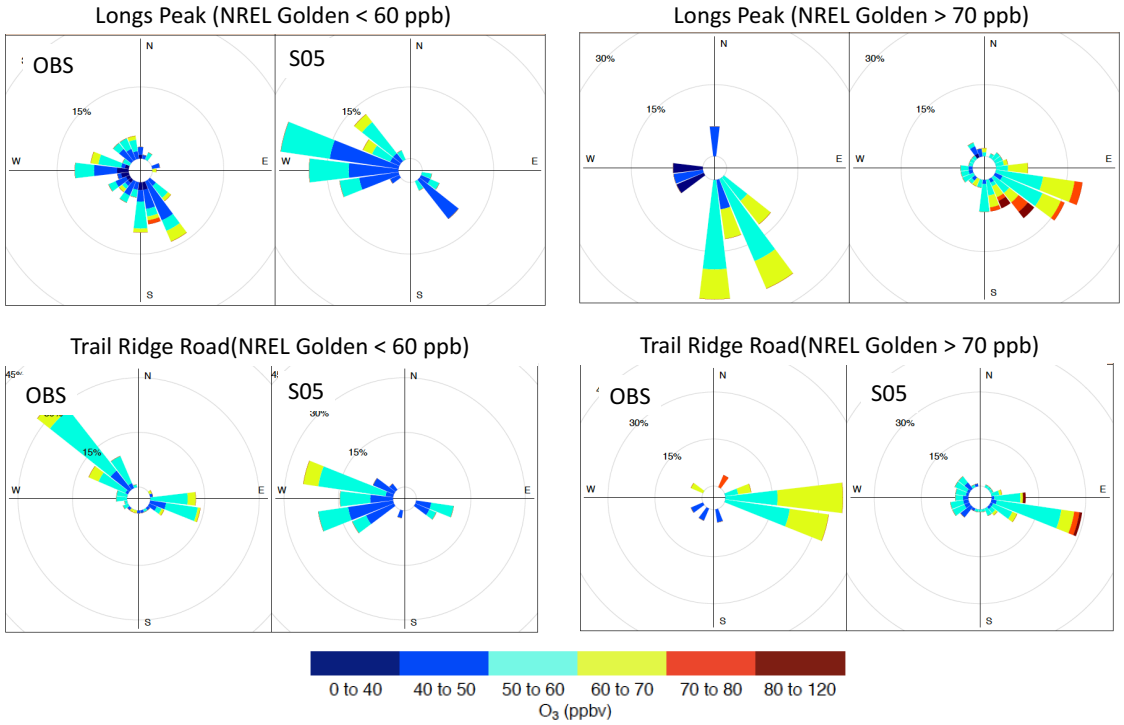

Figure 24: as Figure 22 but for days when NREL Golden mean surface afternoon ozone was < 60 ppb (left columns) or < 70 ppb (right columns)

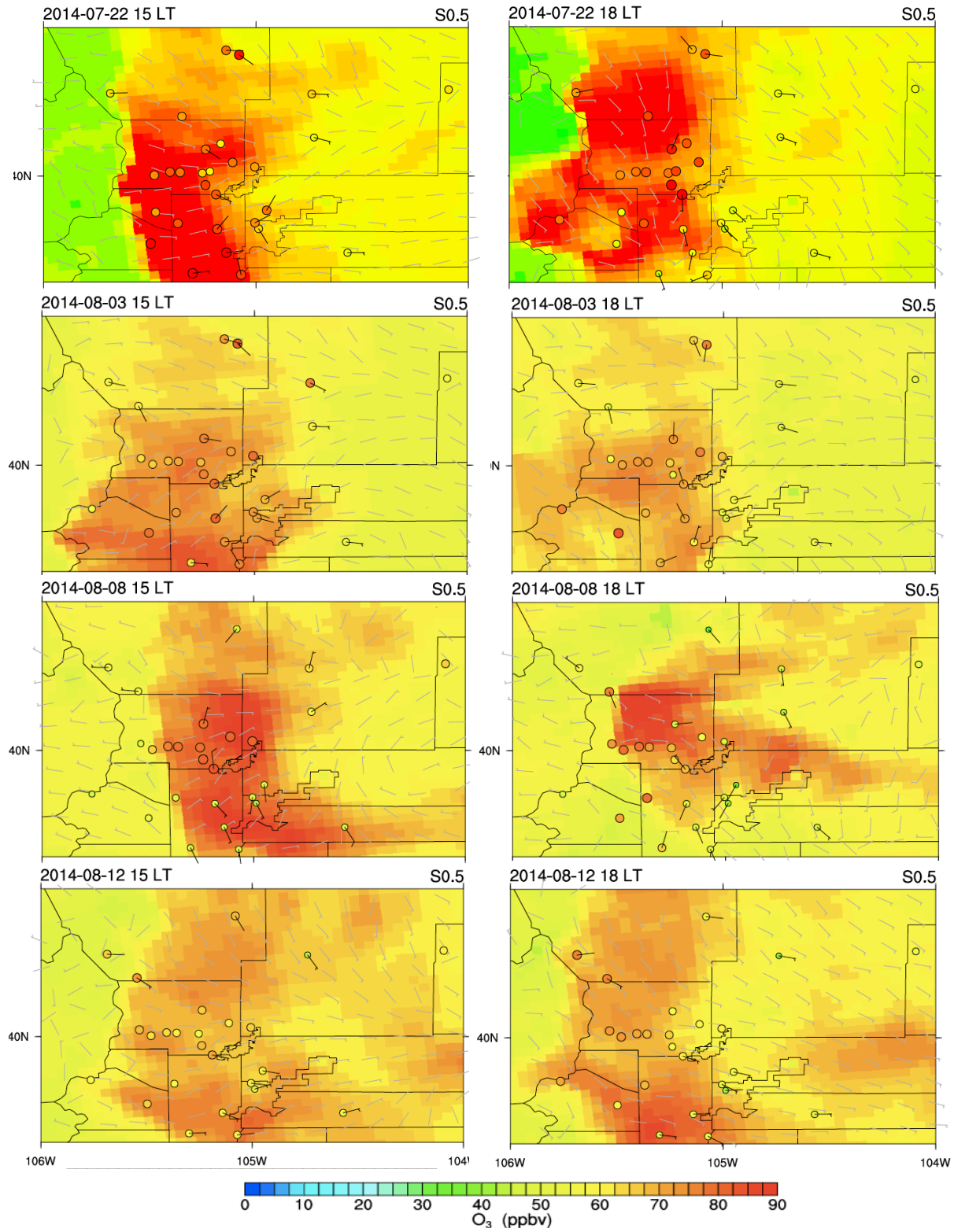

Figure 25: Surface ozone and winds from CMAQ and surface observations for 15 LT and 18 LT on selected days for which observations and model show elevated ozone concentrations.

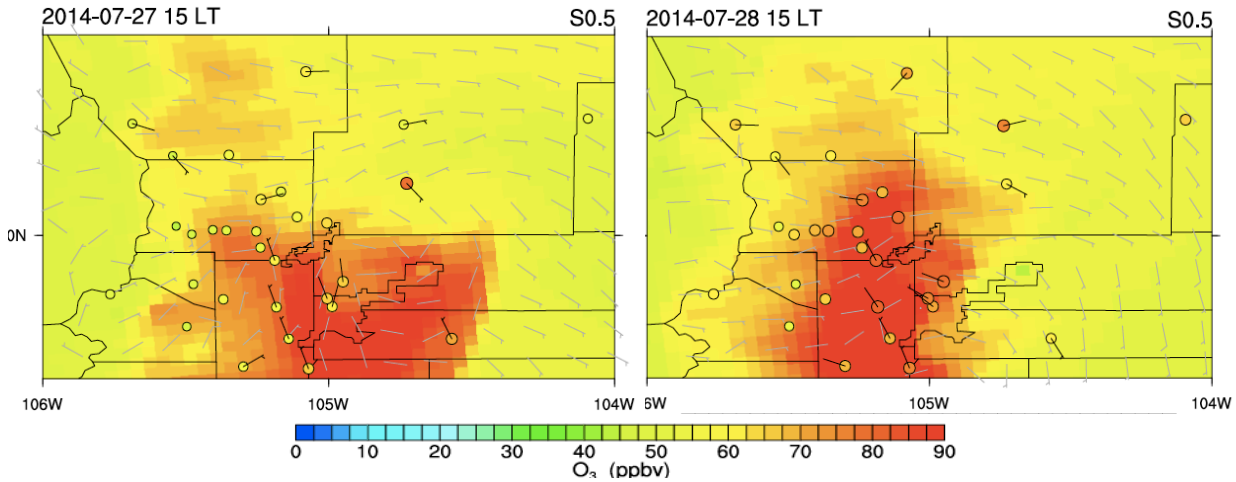

Figure 26: Surface ozone and winds from CMAQ and surface observations for days with a Denver Cyclone. Results for 15 LT are shown.

9 Other Findings

Canister samples collected with the Whole Air Sampler (WAS) from a mobile van have been used in Section 3.1 for evaluating the modeled emission ratios. Most of the cans have been taken near selected emission sources and the data do provide valuable insight into single large emitters. In Table 5 we list the WAS canister samples that showed the ten highest benzene concentrations. Note that the location of some of the samples is incorrect in the file uploaded to the NASA Data Archive. We contacted UC Irvine for providing a correction.

All samples were taken in Weld County as shown in Figure 27. In the same graph, we also show the location of the highest samples; for some locations, more than one sample was taken. In all samples, ethyne concentrations are low suggesting low impact from mobile sources. The highest benzene concentration of 120 ppb (sample 166) was measured near Platteville at a "produced H_2O disposal well" as stated in the canister sampling log sheet. While benzene and also toluene concentrations are very high, typical products released from oil and gas production (e.g. propane and ethane) are not among the highest in this sample. The second highest benzene was measured in samples 206 & 207, which were taken downwind of an oil well waste dumping facility. Samples 12,13 and 14 with benzene concentrations of ~30-40 ppb also show high methane and ethane. These were taken next to the Marilyn Compressor Station, where natural gas is compressed to a specified pressure, thereby allowing it to continue traveling along the pipeline.

The shown samples only provide a snapshot of facilities that where a high release of VOC concentrations was detected during FRAPPÉ and demonstrate a large variability in the composition of the emitted VOCs from the different processes used in oil and gas extraction activities. Some of these sources are not considered in emission inventories nor is the range of VOC emission ratios.

Table 5: WAS Canister samples for the ten highest benzene concentrations.

index	latitude	longitude	CH4_ppmv	Ethane_pptv	Ethyne_pptv	Propane_pptv	Benzene_pptv	Toluene_pptv
166	40.2169	-104.7206	1.93	21,810	259	55,296	120,807	105,708
206	40.3197	-104.5678	2.19	60,643	406	158,469	62,666	48,405
14	40.1453	-104.8694	3.45	141,901	144	92,304	42,686	55,206
207	40.3197	-104.5678	2.17	61,376	347	128,046	36,780	37,423
13	40.1453	-104.8694	3.53	353,178	302	198,842	33,673	92,257
12	40.1453	-104.8694	3.41	335,157	277	190,545	30,864	82,111
25	40.2467	-104.8144	3.10	828,036	313	793,001	24,278	29,512
24	40.2467	-104.8144	3.07	538,869	327	635,712	23,564	28,111
68	40.3647	-104.8328	2.34	303,854	134	399,946	11,668	8,046
5	40.0147	-104.8972	2.84	258,838	641	505,596	8,637	7,194

Figure 27: Location of the ten highest benzene WAS canister samples (top left) and of selected high benzene canister samples with the sample index listed in each graph.

10 Summary

We have employed an extensive range of modeling tools to analyze the data set collected during the FRAPPÉ and DISCOVER-AQ field campaigns. Emphasis was placed on evaluating available emission data against measurements and determining a best-estimate, adjusted emissions scenario which could then be used as a base case for simulating possible emission controls and their impact on photochemical ozone production in the NFRMA.

The WRF/CMAQ model used here captured the general meteorology and resulting tracer transport and mixing very well, given the challenging, terrain induced flow patterns that are typical for summer conditions in this area. Planetary Boundary Layer heights were also generally well simulated, with exceptions on some days. The model did not reproduce well afternoon cloudiness and development of convective storms, resulting, on average, in an overestimate of available photochemically active radiation and resulting ozone production. Many of the high ozone days were simulated very well in the model and the available data on these days allowed for exhaustive evaluation of all aspects of the analysis.

Box models were used to assess the performance of the lumped chemistry schemes that are used in time dependent chemical transport models and we found no strong biases caused by the simplification of the chemistry. Box models and chemical steady state models were also used to inform about the photochemical ozone production regimes across areas of the NFRMA that are dominated by different emission sectors and to support independent verification of conclusions drawn from the WRF/CMAQ zero-out scenarios.

We found that significant adjustments were necessary to the reported emissions from the oil and gas as well as the mobile emission sectors. We recommend that more measurements are made, possibly with CDPHE's new mobile lab, to find possible missing emission sources or identify discrepancies between reported and actual emissions (see below).

Zero-out scenarios were used in both WRF/CMAQ and the box models to determine the influence of the different major emission sectors on regional ozone production, suggesting possible emissions control efforts by the Colorado legislature.

We found that the oil and gas sector as well as the mobile sector are major contributors to NFRMA ozone, with the oil and gas sector influencing more often the northern part of the NFRMA while mobile emissions dominate more in the southern metro area, on average. Large, concentrated NOx emitters such as the power generating stations, DIA, and emissions from some large industrial plants cause a reduction in ozone close to these sources but contribute to ozone production farther downwind, affecting ozone in the western suburbs of the NFRMA and the Foothills during high production days. Prevailing daytime transport to the west during summer exposes the Foothills and Front Range mountains, including Rocky Mountain National Park and, occasionally, the adjacent western valleys to high ozone originating from the NFRMA.

Measures resulting in lowering the emissions from oil and gas as well as from mobile sources could result in substantial reductions of NFRMA ozone. We calculate as much as 10 ppb MDA8 ozone reductions on high ozone days when either sector is zeroed out. These reductions are somewhat spatially separated on classic upslope days while the occurrence of a Denver Cyclone can mix the emissions from both sectors more efficiently resulting in large increases in ozone in Boulder and Gilpin counties. Ozone production in the northern part of the NFRMA is, on

average, more NOx limited while the southern part of the NFRMA is closer to being VOC limited in some places. This places emphasis on NOx availability for efficient ozone production in the Greeley, Loveland and Fort Collins urban areas. NOx emissions inside the Denver-Julesburg basin are particularly important for how efficiently ozone is produced before NOx availability increases due to transport of these air masses across the urban regions to the west. Current emission assessment indicates that lowering NOx emissions in Weld county would have a larger effect on lowering ozone than VOC emission controls from the O&G sector. However, this is only the case if NOx emissions from the mobile sector do not increase in this area, which could be the case given the increasing push of suburban development into the eastern sections of the NFRMA. Because the evaluation of the NOx emissions in the region is difficult, mainly because of the short atmospheric lifetime and the distribution of large point sources, the NOx budget is one of the most uncertain parameters in this analysis.

Measures resulting in the lowering of mobile emissions would reduce ozone everywhere in the NFRMA, emphasizing the western and southwestern sectors of the region.

NOx reductions from the EGUs in the area (shutdown of the Valmont plant and conversion of the last boiler of the Cherokee plant to natural gas) will result in localized increases of ozone (but also lower the NO_2 concentrations there), but will help lower ozone somewhat in the western suburbs.

Industrial VOC emissions appear less important compared to mobile and O&G on the large scale, but can be very important locally, such as in Commerce City. Overall reductions in industrial emissions would only have a small impact on some of the western suburbs, although somewhat larger than that from the EGU emissions.

The Foothills communities and Wilderness areas in the Mountains and adjacent western valleys would generally benefit from a reduction of emissions in the NFRMA as this would result in less advected ozone from the NFRMA as well as less additional production during air mass transport.

We have identified a number of point sources which, at the time of measurement, emitted alarming amounts of highly reactive and toxic VOC. Some of these sources were not part of the emission inventory. From the sporadic observations made during FRAPPÉ it is impossible to tell what fraction these sources contribute to the derived adjustments to the VOC emissions in the oil and gas sector, for example. Better constrained emission inventories would help State Implementation Plan (SIP) modeling efforts and greatly aid the process of developing effective ozone reduction strategies.

Finally, since emissions in the NFRMA are constantly evolving, due to rapid population growth causing ever increasing commuting miles driven as well as impacting transport of goods in and out of the area, and due to market driven rapid changes in the oil and gas extraction activity in the region, repeated aircraft measurements like what was done during FRAPPÉ would greatly help to detect these trends, now that a baseline has been established with the 2014 campaign.

11 FRAPPÉ Website, Meetings and Public Outreach

We have been updating the NCAR/ACOM FRAPPÉ Website on a regular basis (https://www2.acom.ucar.edu/frappe). To the Best of our knowledge the list of publications on the website represent the latest published papers. Numerous other publications have been submitted to journals and will be added to the website as soon as they have undergone the peer-review process.

In May 2017, we organized a joint FRAPPÉ and DISCOVER-AQ Science Team Meeting. All presentations have been made available on the NCAR/ACOM FRAPPÉ website. As part of the Science Team Meeting and in recognition of the EPA Air Awareness Week NCAR held an Air Quality Fair at the NCAR Mesa Lab with booth by NCAR, CU, RAQC, EPA, GO3, NPS, Ball Aerospace and many others.

Presentations have been given to Policy Makers and AQ Managers on the progress of FRAPPÉ analysis. The more recent presentations include talks at the Colorado Air Quality Control Commission (AQCC) Spring 2017 Science Forum, the Air & Waste Management Association (AWMA) in November 2016 and a presentation to the Air Pollution Control Commission (APCC) in August 2016. The authors will be available to consult with CDPHE if questions arise with respect to the materials made available and results presented here, and are available to present and discuss the results and findings from this report at upcoming CDPHE or related meetings if requested.

More recent public outreach activities included NCAR Earth Explorer Talks at the Boulder Mesa Lab in January 2017 and the Denver Library in June 2017. A recording of the Boulder Talks is available from the UCAR Connect Youtube site: https://www.youtube.com/watch?v=kCPzUFaWwBs)

12 Data and Tool Availability

The tools and data sets used in this report are publicly available.

- BOXMOX: http://boxmodeling.meteo.physik.uni-muenchen.de/index.html
- CMAQ: https://www.cmascenter.org/cmaq/
- SMOKE: https://www.cmascenter.org/smoke/
- FRAPPÉ and DISOVER-AQ Data Set: https://www-air.larc.nasa.gov/missions/discover-aq/discover-aq.html
- WRF Modeling System: http://www2.mmm.ucar.edu/wrf/users/

We offer to make all graphs included in this report available as electronic version. In addition, we can provide a full set of additional graphs including model comparisons to daily C-130 and P-3 flights, daily maps of measured and modeled surface ozone and similar. We further will provide, upon request, all analysis codes (mostly written in NCL and R), as well as the CMAQ a priori and S0.5 emission inputs, the WRF ADP/FRAPPÉ nudging model output and the S0.5 CMAQ model output or any other data set. Given the large data volume involved, however, we consider it the most feasible to receive input from the State on the requested set of information and discuss on the appropriate method for the data exchange, which will be decided on dependent on the requested amount of data.

We thank the FRAPPÉ and DISCOVER-AQ Science Team for the collection, quality control and availability of the observational data sets. Due to the wealth of data set included in this report we are not able to list each data PI individually. All observations included in this report have been downloaded from the publicly available NASA FRAPPÉ/DISCOVER AQ Data Archive (https://www-air.larc.nasa.gov/missions/discover-aq/discover-aq.html). Each data set contains the contact information for the data PI. We acknowledge the State of Colorado/CDPHE and the National Science Foundation (NSF) for funding of FRAPPÉ. NASA is acknowledged for funding DISCOVER-AQ.

References

Baumann, K., E. J. Williams, J. A. Olson, J. W. Harder, and F. C. Fehsenfeld (1997), Meteorological characteristics and spatial extent of upslope events during the 1993 Tropospheric OH Photochemistry Experiment, J. Geophys. Res., 102(D5), 6199–6213, doi:10.1029/96JD03251.

Benedict, K. B., Carrico, C. M., Kreidenweis, S. M., Schichtel, B., Malm, W. C. and Collett, J. L. (2013), A seasonal nitrogen deposition budget for Rocky Mountain National Park. Ecological Applications, 23: 1156–1169. doi:10.1890/12-1624.1

Brodin, M., D. Helmig, S. Oltmans (2010), Seasonal ozone behavior along an elevation gradient in the Colorado Front Range Mountains. Atmospheric Environment 44 :5305-5315

Brodin, M., D. Helmig, B. Johnson, and S. Oltmans (2011), Comparison of ozone concentrations on a surface elevation gradient with balloon-borne ozonesonde measurements. Atmos. Environ., 45, 5431- 5439.

Darrouzet-Nardi, A., J. Erbland, W. D. Bowman, J. Savarino, and M. W. Williams (2012), Landscapelevel nitrogen import and export in an ecosystem with complex terrain, Colorado Front Range. Biogeochemistry, 109, 271-285.

Doran, J.C. (1996), The influence of Canyon Winds on flow fields near Colorado's Front Range, J. Appl. Meteorology, Volume 35, 587-600.

Greenland, D. (1980), The Climate of Niwot Ridge, Front Range, Colorado, U.S.A., Arctic and Alpine Research, vol. 21, no. 4, 1989, pp. 380–391., www.jstor.org/stable/1551647.

Haagenson, P. L., (1979), Meteorological and climatological factors affecting Denver air quality, Atmos. Environ., 13, 79–85.

Johnson, R.H. and J.J. Toth (1982), Topographic effects and weather forecasting in the Colorado PROFS mesonetwork area, Preprint Volume: 9th Conference on Weather Forecasting and Analysis, June 28 - July 1, 1982; Seattle, WA, 440-445.

Olson, J. A., K. Baumann, C. J. Volpe, J. W. Harder, E. J. Williams, and G. H. Mount (1997), Meteorological overview of the 1993 OH Photochemistry Experiment, J. Geophys. Res., 102(D5), 6187–6197, doi:10.1029/96JD00402.

Olson, J. R., Crawford, J. H., Chen, G., Brune, W. H., Faloona, I. C., Tan, D., Harder, H., and Martinez, M. (2006), A reevaluation of airborne HOx observations from NASA field campaigns, J. Geophys Res., 111 D10301, doi:10.1029/2005JD006617.